Metals geochemistry and ecological risk assessment in a tropical mangrove (Can Gio, Vietnam)

Nguyen Thành-Nho, Cyril Marchand, Emilie Strady, Truong-Van Vinh, Tran-Thi Nhu-Trang

Metals geochemistry and ecological risk assessment in a tropical mangrove (Can Gio, Vietnam)

Nguyen Thanh-Nho[1,2], Cyril Marchand[1,2,*], Emilie Strady[3,4], Truong-Van Vinh[2,5], Tran-Thi Nhu-Trang[1,6]

1. Department of Analytical Chemistry, Faculty of Chemistry, University of Science, Vietnam National University- Ho Chi Minh City

2. IMPMC, Institut de Recherche pour le Développement (IRD), UPMC, CNRS, MNHN, Noumea New Caledonia, France.

3. Univ. Grenoble Alpes, CNRS, IRD, Grenoble INP, IGE, F-38000 Grenoble, France*

4. CARE-HCMUT, Ho Chi Minh City, Vietnam

5. Nong Lam University, Ho Chi Minh City, Vietnam

6. Faculty of Chemical Engineering and Food Technology, Nguyen Tat Thanh University, Vietnam.

* *Corresponding author: Cyril.marchand@ird.fr*

ABSTRACT

Mangrove sediments act as natural biogeochemical reactors, modifying metals partitioning after their deposition. The objectives of the present study were: to determine distribution and partitioning of metals (Fe, Mn, Ni, Cr, Cu, Co and As) in sediments and pore-waters of Can Gio Mangrove; and to assess their ecological risks based on Risk Assessment Code. Three cores were collected within a mudflat, beneath *Avicennia alba* and *Rhizophora apiculata* stands. We suggest that most metals had a natural origin, being deposited in the mangrove mainly as oxyhydroxides derived from the upstream lateritic soils. This hypothesis could be supported by the high proportion of metals in the residual fraction (mean values (%): 71.9, 30.7, 80.7, 80.9, 67.9, 53.4 and 66.5 for Fe, Mn, Ni, Cr, Cu, Co, and As respectively, in the mudflat). The enrichment of mangrove-derived organic matter from the mudflat to the *Rhizophora* stand (i.e. up to 4.6 % of TOC) played a key role in controlling metals partitioning. We suggest that dissolution of Fe and Mn oxyhydroxides in reducing condition during decomposition of organic matter may be a major source of dissolved metals in pore-waters. Only Mn exhibited a potential high risk to the ecosystem. Most metals stocks in the sediments were higher in the *Avicennia* stand than the *Rhizophora* stand, possibly because of enhanced dissolution of metal bearing phases beneath later one. In a context of enhanced mangrove forests destruction, this study provides insights on the effects of perturbation and oxidation of sediments on metal release to the environment.

Keywords: Mangrove; Sequential extraction; Metal geochemistry; Partitioning; Ecological risk; Vietnam.

1. Introduction

Mangrove ecosystems are closely tied to anthropogenic activities. Due to their specific characteristics, i.e. their richness in fine particles and organic matter, mangrove sediments can act as natural sinks for metals originating from natural and anthropized watersheds (Clark et al. 1998, Marchand et al. 2011a, Tam and Wong 1996). In mangrove sediments, the partitioning of metals between different phases, i.e. organic matter, iron-manganese oxyhydroxides, sulphides, carbonates (Tam and Wong 1996, Zhang et al. 2014) is strongly influenced by sediment characteristics, i.e. pH, redox potential, particle size (Otero et al. 2009). Accordingly, the mangrove zonation, the hydrological conditions and the presence of different tree species will influence the above characteristics (Marchand et al. 2004, Marchand et al. 2003) which will in turn influence metal accumulation and speciation in the sediments. In fact metals can be released from sediments into pore-waters in suboxic/anoxic conditions by the dissolution of bearing phases (Chakraborty et al. 2016, Marchand et al. 2012) during diagenetic processes, which can subsequently re-precipitate with another bearing phase (Noël et al. 2014). Then, dissolved metals can be exported to adjacent surface waters (Holloway et al. 2016, Sanders et al. 2012) and also be transferred to mangrove's living organism such as fishes, crabs, snails and mangrove's leaves and roots (Chakraborty et al. 2014, De Wolf and Rashid 2008, Parvaresh et al. 2011). In a context of enhanced mangrove forests destruction at a worldwide scale i.e. at a rate close to 1 % per year (Duke et al. 2007), the perturbation and oxidation of sediments can induce the dissolution of sulfide minerals, which can result in sediment acidification (Dent 1986) and can enhance the release of metals from the sediment into the aquatic environment. Thus, the understanding of metal behaviors in mangrove ecosystems is highly relevant for the environment itself but also for human, as mangroves provide important ecosystem services (Lee et al. 2014, M. Brander et al. 2012).

In Vietnam, large mangrove areas were devastated by herbicide mixture during the war in the 70's, and the Can Gio Mangrove was one of the most heavily sprayed areas (Hong 2001, Ross 1975). However, mangrove restoration efforts have been realized and almost 40 years after, the rehabilitated mangrove is now more diverse in community structure than prior to the war (Hong

2001). Nowadays, this mangrove is largely dominated by *Rhizophora apiculata* and *Avicennia alba* species, the latter one developing at lower elevation along tidal creek. The Can Gio Mangrove is located downstream Ho Chi Minh City, the economic capital of Vietnam with almost 10 million inhabitants. Mangrove river network acts as a unique gate for water outlet from Ho Chi Minh City to the South China Sea. Industrial activities, economic developments and rapid population growth are inducing high pressure on water and sediment quality of the adjacent river, the Sai Gon River (Babut et al. 2019, Nguyen et al. 2018, Strady et al. 2017). Strady et al. (2017) stated that the main rivers and canals in the city were moderately contaminated by major metal(oid)s. Recently, Thanh-Nho et al. (2018) highlighted that metals can be transferred over long distance from upstream to the mangrove forest, and that elevated inputs of metals in the estuary were the result of enhanced runoff and soil leaching during the monsoon season. Consequently, taking into account the mangrove specific geochemical characteristics, the lack of wastewater treatment plants in emerging countries as Vietnam and the important local ecosystem services provided by the Can Gio Mangrove (Cormier-Salem et al. 2017, Kuenzer and Tuan 2013), more attention should be paid on metals distribution, speciation, bioaccumulation and transfer in mangrove ecosystems. We note that so far, in the Can Gio Mangrove, only total metal concentrations in surface water, suspended sediment and surface sediment were investigated (Costa-Boddeker et al. 2017, Thanh-Nho et al. 2018) and the evaluation of the metal speciation in the sediment has not yet been assessed. It can be evaluated by the technique of sequential extraction (Tessier et al. 1979) which provides a classification of metals bound to different geochemical fractions. This technique also allow to characterize the diagenetic processes taking place in the sediment over a depth profile and to characterize the geogenic components and so origin of the sediments.

Within this context, the objectives of this study were: *i)* to investigate the geochemistry of Fe, Mn, Ni, Cr, Cu, Co and As in sediment cores of the Can Gio Mangrove by focusing on the metal speciation in the sediments and their concentrations in pore-waters; and *ii)* to assess the potential ecological risks of these metals accumulated in the sediments on the mangrove ecosystem by using Risk Assessment Code (Benson et al. 2017). The sediment cores were sampled on three specific

environments characterized by different elevation (i.e. tidal inundation), organic matter content, redox stratification and plant cover: in the mudflat, beneath *Avicennia* stand and beneath *Rhizophora* stand.

2. Materials and methods

2.1. Study site

The Can Gio Mangrove (approximately 35,000 ha, extending from 10º22'-10º44'N and 106º46'-107º01'E (Tuan and Kuenzer 2012)) is located in the south of Vietnam, at the downstream part of the Sai Gon and Dong Nai Rivers watershed and in the South China Sea coastal zone (Fig. 1). It is a Biosphere Reserve of UNESCO since 2000 and it is also a well-known example of "mangrove afforestation and reforestation area'' (Blasco et al. 2001). The Can Gio Mangrove is home to more than 20 mangrove species with two dominant ones: *Rhizophora apiculata* and *Avicennia alba* (Luong et al. 2015), and 200 species of fauna (e.g. amphibians, fishes, benthic organisms, etc.). The main economic activities of the local people are forest management, aquaculture, fishing and salt production (Kuenzer and Tuan 2013). The Can Gio Mangrove is subject to the typical tropical monsoon climate, with two distinct seasons. The dry season lasts from November to April and the monsoon season from May to October. The annual mean precipitation is about 1,300 to 1,400 mm, with ~ 90 % of the precipitation falling during the monsoon season and the annual mean temperature ranges from 26.5 °C to 30 °C. It is also subject to a semi-diurnal tidal regime. The topography of the Can Gio Mangrove is generally low-lying. Average vertical accretion rates in the Can Gio Mangrove are similar between fringe (1.06 ± 0.12 cm $year^{-1}$) and interior mangrove (0.99 ± 0.09 cm $year^{-1}$) (MacKenzie et al. 2016). The sediment is composed of alluvial deposits and lateritic soils (Luong 2011) from the Sai Gon and Dong Nai Rivers. The lateritic soils originate from the physico-chemical weathering of basaltic rocks in the Central Highland of Vietnam (Egawa and Ooba 1963).

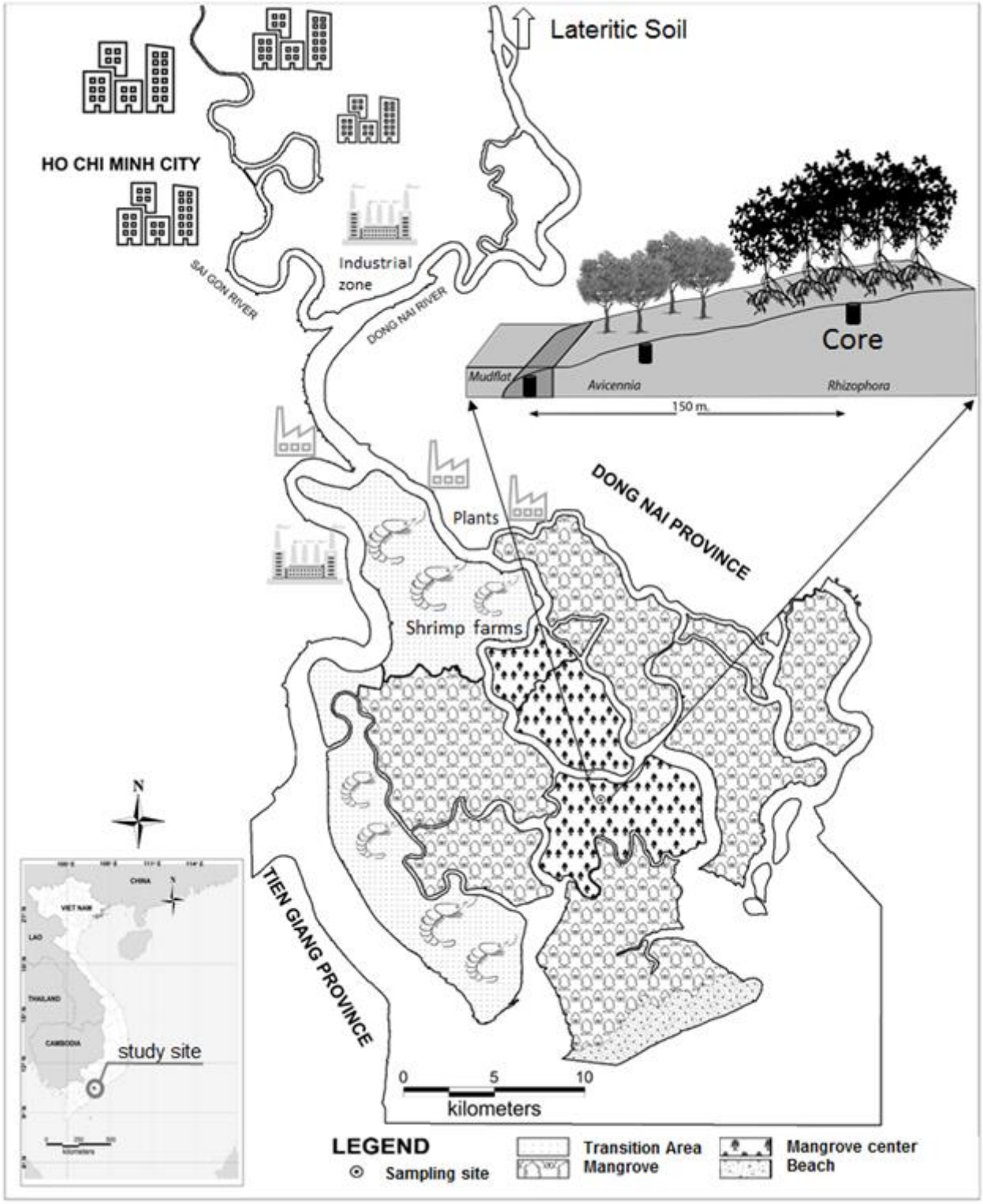

Fig. 1. Location of the Can Gio Mangrove and the three cores (90 cm depth) collected in the mudflat, beneath the Avicennia stand and the Rhizophora stand.

2.2. Sample collections and preservations

Sampling was carried out in the center area of the Can Gio Mangrove during the monsoon season (October 2016). Three cores (90 cm depth) were collected with an Eijkelkamp gouge auger at low tide in the mudflat (lower elevation than the mangrove stands), beneath an *Avicennia alba*

stand and a *Rhizophora apiculata* stand (Fig. 1). Cores were immediately sectioned into 10 samples: every 5 cm from the surface to 30 cm depth, every 10 cm from 30 to 50 cm depth, and every 20 cm from 50 to 90 cm depth. Samples were stored in polythene bags, preserved in a cooler box for their transfer to the laboratory and were then stored frozen (-20 °C) until drying. Dried samples were grinded using an agate pestle and mortar, and sieved using 100 µm pore size for sequential extraction of metals fractions and for total organic carbon (TOC) analysis.

For dissolved metal analysis, pore-waters were extracted on the day of coring with soil moister sampler Rhizon®, which were directly inserted into the center of the cores (Marchand et al. 2012). All samples were then filtered through 0.45 µm Sartorius® filter membranes and acidified to pH < 2 by Suprapur® concentrated HNO_3 (Merck). The samples were then preserved in cleaned 14 ml polypropylene (PP) tubes at 4 ^{o}C until analysis.

2.3. Analytical methods and calculations

2.3.1. Salinity, pH and redox measurements

Additional cores beneath each mangrove stand and in the mudflat were collected to measure salinity, pH and redox. These parameters were measured in-situ. Salinities were determined using an ATAGO refractometer (S-10, Japan) after extracting a drop of pore-water from each sediment layer. pH was measured using a glass electrode (pH 3110-WTW), which was pre-calibrated using pH 4, 7 and 10 standard buffer solutions (NIST scale). Redox potential was measured using digital voltmeter with Pt and Ag/AgCl (reference) electrode connected to pH/mV/T meter (pH100-YSI), which was periodically checked using 0.43V standard solution and deionized water. Redox data are reported relative to a standard hydrogen electrode i.e. after adding 194 mV to the original mV values obtained with an Ag/AgCl (reference electrode) at 30 ^{o}C. The redox scale was fully described by Marchand et al. (2011a), as follows: (i) oxic > 400 mV, containing measurable dissolved oxygen; (ii) 100 mV < suboxic < 400 mV, with a lack of measurable oxygen or sulfide, containing dissolved iron or manganese, with no reduction of sulfate; (iii) anoxic < 100 mV, with sulfate reduction.

2.3.2. Metal concentrations in pore-waters

166 Dissolved Fe, Mn, Ni, Cr, Cu, Co and As concentrations were directly measured by Thermo
167 Scientific iCAPQ ICP-MS with a Kinetic Energy Discrimination-Argon Gas Dilution module
168 (KED - AGD mode) (Kutscher et al. 2014) using internal standard calibration (AETE-ISO platform,
169 OSU-OREME/Université de Montpellier). Accuracy and precision were controlled using the
170 certified reference material SLEW-3 (Table 1a).

171 *Table 1. Quality control of analytical methods applied for dissolved and total metals concentrations analysis*
172 *respectively: a) accuracy, precision and detection limit using estuarine water SLEW-3; b) total metal concentrations*
173 *were calculated by summing the four single fraction (F1 + F2 + F3 + F4) from CRM (BCR-277R).*

174 *a) Dissolved metal concentration analysis.*

Element	*Detection limit (µg L^{-1})*	*Certificated values of SLEW-3 (µg L^{-1})*	*Measured values (µg L-1)*	*Recovery (%)*	*Relative standard deviation (%)*
Fe	0.031	0.568 ± 0.059	0.661 ± 0.073	116	11
Mn	0.013	1.61 ± 0.22	1.469 ± 0.016	91	1
Ni	0.011	1.23 ± 0.07	1.230 ± 0.014	100	1
Cr	0.022	0.183 ± 0.019	0.0182 ± 0.020	99	11
Cu	0.011	1.55 ± 0.12	1.491 ± 0.041	96	3
Co	0.0092	0.042 ± 0.010	0.0464 ± 0.0025	110	5
As	0.0062	1.36 ± 0.09	1.569 ± 0.013	115	1

175 *b) Total metal concentration analysis*

Element	Certificated values of *BCR-277R* (mg kg^{-1})	Measured values (mg kg^{-1}, n = 9)	Recovery (%)	Relative standard deviation (%)	Analytical method
Fe	NA	50,843 ± 3,029	-	5.8	FAAS
Mn	NA	897 ± 37	-	4.2	FAAS
Ni	130 ± 8	125.9 ± 6.1	96.9	4.9	ICP-MS
Cr	188 ± 14	179.9 ± 16.1	95.7	9	ICP-MS
Cu	63 ± 7	58.9 ± 4.6	93.6	7.9	ICP-MS
Co	22.5 ± 1.4	23.1 ± 1.7	102.6	7.5	ICP-MS
As	18.3 ± 1.8	18.1 ± 1.5	98.9	8.2	ICP-MS

176 *2.3.3. Sequential extraction: metal fractions*

177 To evaluate the geochemistry and availability of metals (Fe, Mn, Ni, Cr, Cu, Co and As) in the
178 sediment cores, a sequential extraction procedure was carried out based on the method developed
179 by Tessier et al. (1979) and Ure et al. (1993). Each element was divided into four operationally-
180 defined geochemical fractions: exchangeable/carbonate fraction (acid-soluble phase), Fe – Mn
181 oxides fraction (reducible phase), organic fraction (oxidizable phase) and a residual fraction.
182 Briefly, the various single extractions were performed as following: 1 g of fine dry sediments were

put into 50 mL PP tubes with caps, which were also used for shaking time and centrifugation to minimize the possible loss of the centrifuge – washing step. For the determination of the acid-soluble fraction (F1), we used 8 mL of 1 M buffer acidic solution (CH_3COOH/CH_3COONH_4, pH = 5) at room temperature during 5 h; for the reducible fraction (F2), we used 20 mL of 0.04 M $NH_2OH.HCl$ in 25 % CH_3COOH (*m/v*) at 96 ^oC during 6 h; for the oxidizable fraction (F3), we used 3 mL of 0.02 M HNO_3 and 8 mL of 30 % H_2O_2. 5 mL of 3.2 M CH_3COONH_4 was added into the solution to prevent reabsorb of these metals onto particles surface; for the total metals concentration in the residual fraction (F4), the samples was digested using 10 mL of concentrated HNO_3/HCl/HF (3:1:1 = *v/v*) in polytetrafluoroethylene (PTFE) vessel at 110 ^oC for 48 h. After cooling, 2 mL of concentrated HNO_3 (n = 2) was added into these samples for eliminating residual HF. For each adding, the solution were evaporated near to dryness at 160 ^oC. The samples were filtrated and adjusted using deionized water into 25 mL, and were then stored in pre-cleaned polypropylene tubes at 4 ^oC until analysis.

2.3.4. Total metal concentration

Total metal concentrations were obtained by summing the four single fractions (F1 + F2 + F3 + F4). The quantifications of Fe and Mn concentrations were performed by Flame Atomic Absorption (Shimadzu AA-6650) while the other metals (Co, Ni, Cu, As and Cr) were analyzed by ICP-MS (Agilent 7700x) using spiked ^{103}Rh and ^{197}Au as internal standard (Table 1b). The analytical precision and accuracy were insured by analyzing certified reference material estuarine sediment (BCR-277R) intercalated in each batch of sample digestion. All reagents were analysis grade (Merck) and all containers were de-contaminated by soaking in 5 % nitric acid for 24 h and rinsed in deionized water.

2.3.5. Total organic carbon (TOC)

TOC analysis was carried out on a Shimadzu® TOC-L series analyzer combined with a solid sample module (SSM-5000A) heating at 900 ^oC. Glucose standard (40 %, Sigma Aldrich) was used for calibrations. Repeated measurements of the standards at different concentrations indicated a measurement deviation < 2 %.

2.3.6. Sediment bulk density and metal stock estimation

The bulk density is defined as the ratio of dry sediment mass to sediment volume (including pore space) and is typically expressed in g cm^{-3}. The sediment bulk density was calculated for each layer (i.e. every 5 cm from 0 to 30 cm depth and every 10 cm from 30 to 50 cm depth) of the three cores (i.e. the mudflat, the *Avicennia* and the *Rhizophora* stands) by taking subsamples of known volume sediment, drying them at 45°C during 24h and by weighing them.

The determination of the metal stocks may help to understand if a mangrove stand can be a sink or a source of metals, by taking into account that diagenetic processes influence the stocks. Considering that the stands develop very close to each other (with the same sediment inputs), the difference of metals stocks between them should be related to diagenetic processes, to dissolution of bearing phases, and thus to metals export to adjacent tidal creek and/or subject to plant uptake. Thus, the metal stocks present in the Can Gio Mangrove sediment were estimated from the average total metal concentrations and average bulk density determined in each core from surface to 50 cm depth (e.g. the depth was chosen at 50 cm depth in order to compare it to the estimated stocks from the literature), according to the following equation.

$$\text{Metal Stock (t ha}^{-1}) = (C_{sediment} * BD * 50 * 100)/10^6$$

where:

$C_{sediment}$: average total metal concentration in the upper 50 cm (mg kg^{-1})

BD: average bulk density in the upper 50 cm (g cm^{-3})

50: length of the core used for estimation of metal stock (cm)

100: conversion factor from g cm^{-2} to t ha^{-1}

10^6: conversion factor of a metal concentration in mg kg^{-1}

2.3.7. Data analysis

Pearson correlation coefficients were performed using statistical package software (SPSS: version 23) to identify major relationships between metal concentrations and physico-chemical parameters as well as interrelationships between metals together.

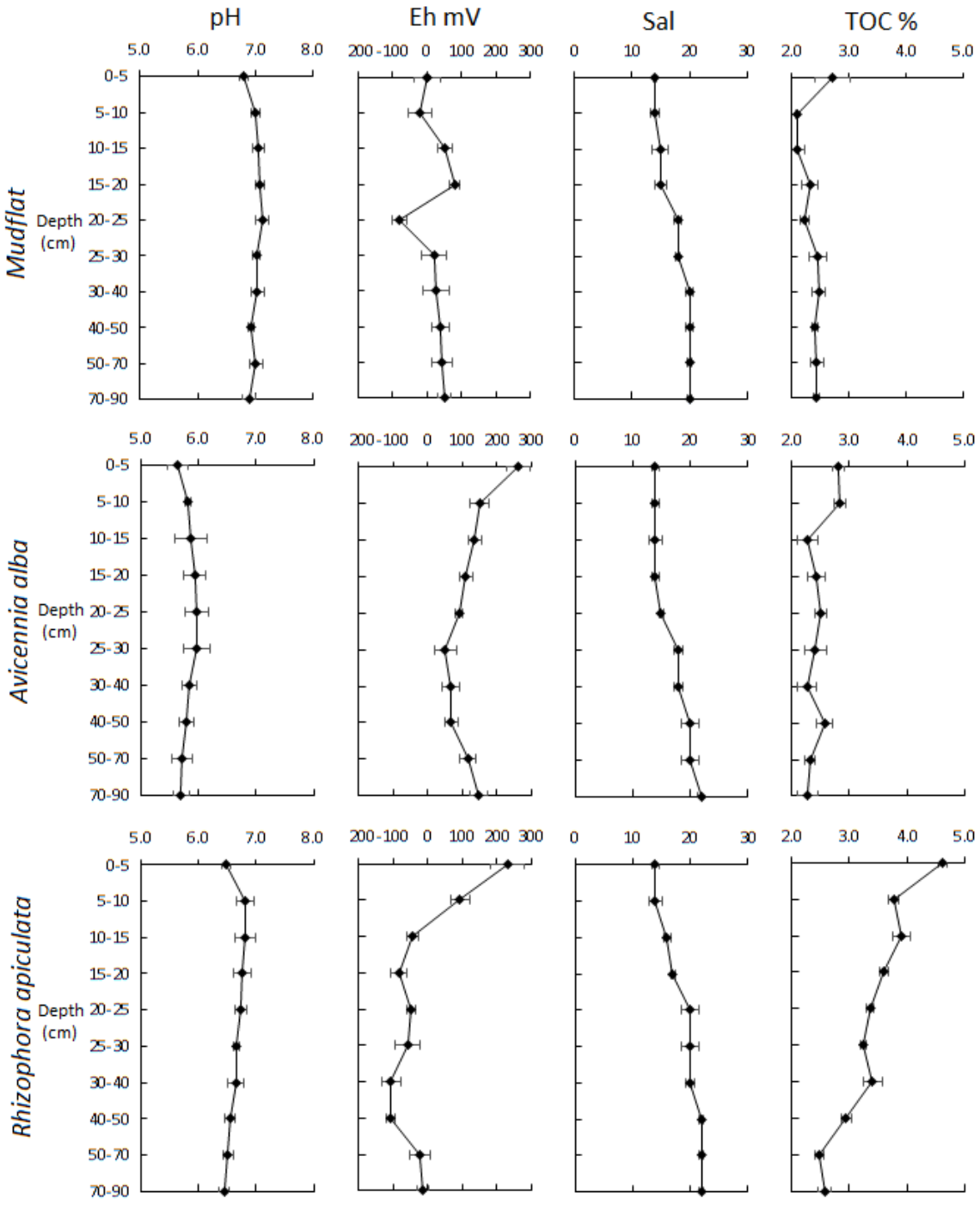

Fig. 2. Depth distributions of pH, Eh, Salinity and TOC in the mudflat, the Avicennia and the Rhizophora stands in the Can Gio Mangrove.

3. Results

3.1. Physico-chemical parameters in the sediment cores

The depth evolutions of pH, redox potential (Eh), salinity and total organic carbon (TOC) in the mudflat and the mangrove stands are presented in Fig. 2. pH was stable with depth whatever the sites, being lower in the *Avicennia* stand (5.6 to 6.0) than in the *Rhizophora* stand (6.5 to 6.8) and in the mudflat (6.8 to 7.1). Eh distributions and values differed in the three environments. The

mudflat was characterized by anoxic condition in whole core, ranging between 73 mV and -88 mV. The sediments beneath mangroves stands were characterized from suboxic to anoxic conditions toward the bottom of the cores. In the *Avicennia* stand, Eh values decreased from 254 mV at the top of the core to 43 mV at 30 cm depth, and then slightly increased without being higher than 140 mV. In the *Rhizophora* stand, redox values decreased from the top of the core (224 mV) to 20 cm depth (- 90 mV) and then fluctuated between of -20 mV to -115 mV. Salinity increased with depth in the three cores with similar distribution patterns, from 14 to 22. TOC contents varied with depth in the mudflat (from 2.7 % to 2.1 %) and in the *Avicennia* stand (from 2.8 % to 2.3 %) without specific distributions patterns, while in the *Rhizophora* stand TOC concentrations were higher than in the other sites, and decreased with depth (from 4.62 % to 2.1 %).

3.2.Total metal concentrations in the sediment cores

The total metal concentrations (Fe, Mn, Ni, Cr, Cu, Co and As) in the three cores were obtained by summing the four single fraction (i.e. F1 + F2 + F3 + F4). The depth's distribution of each metal in the mudflat, the *Avicennia* stand, the *Rhizophora* stand and their mean concentrations are presented in Fig. 3 and supplementary data (Table SD).

Total Fe concentrations did not exhibit specific distribution with depth in the three environments. The mean values of total Fe concentration decreased from the mudflat (53,146 ± 1,422 mg kg^{-1}) to the mangrove stands (49,305 ± 2,198 mg kg^{-1} and 47,135 ± 2,370 mg kg^{-1} in the *Avicennia* stand and *Rhizophora* stand, respectively). The total Mn concentrations decreased with depth in each environment, from 653 mg kg^{-1} to 310 mg kg^{-1} in the mudflat, from 800 mg kg^{-1} to 227 mg kg^{-1} in the *Avicennia* stand and from 350 mg kg^{-1} to 160 mg kg^{-1} in the *Rhizophora* stand. Total Ni and Cr concentrations presented small amplitude with depth in the three environments but their mean concentrations in each core evidenced higher mean values in the *Avicennia* and *Rhizophora* stands (62.5 ± 2.6 mg kg^{-1} and 61.1 ± 1.7 mg kg^{-1} for Ni; 95.3 ± 1.4 mg kg^{-1} and 95.8 ± 4.2 mg kg^{-1} for Cr, respectively) than in the mudflat (52.7 ± 3.7 mg kg^{-1} for Ni and 86.6 ± 3.8 mg kg^{-1} for Cr). Total Co concentrations showed similar distributions between environments, being stable values in the upper horizons from 0 to 40 cm depth and then increasing to reach a maximum

values of 24.2 mg kg^{-1}, 29.7 mg kg^{-1} and 25.8 mg kg^{-1} in the mudflat, the *Avicennia* stand and the *Rhizophora* stand, respectively. Finally, total As and Cu concentrations did not present any specific vertical distribution patterns, and their mean concentrations were similar to all environments (supplementary data, Table SD).

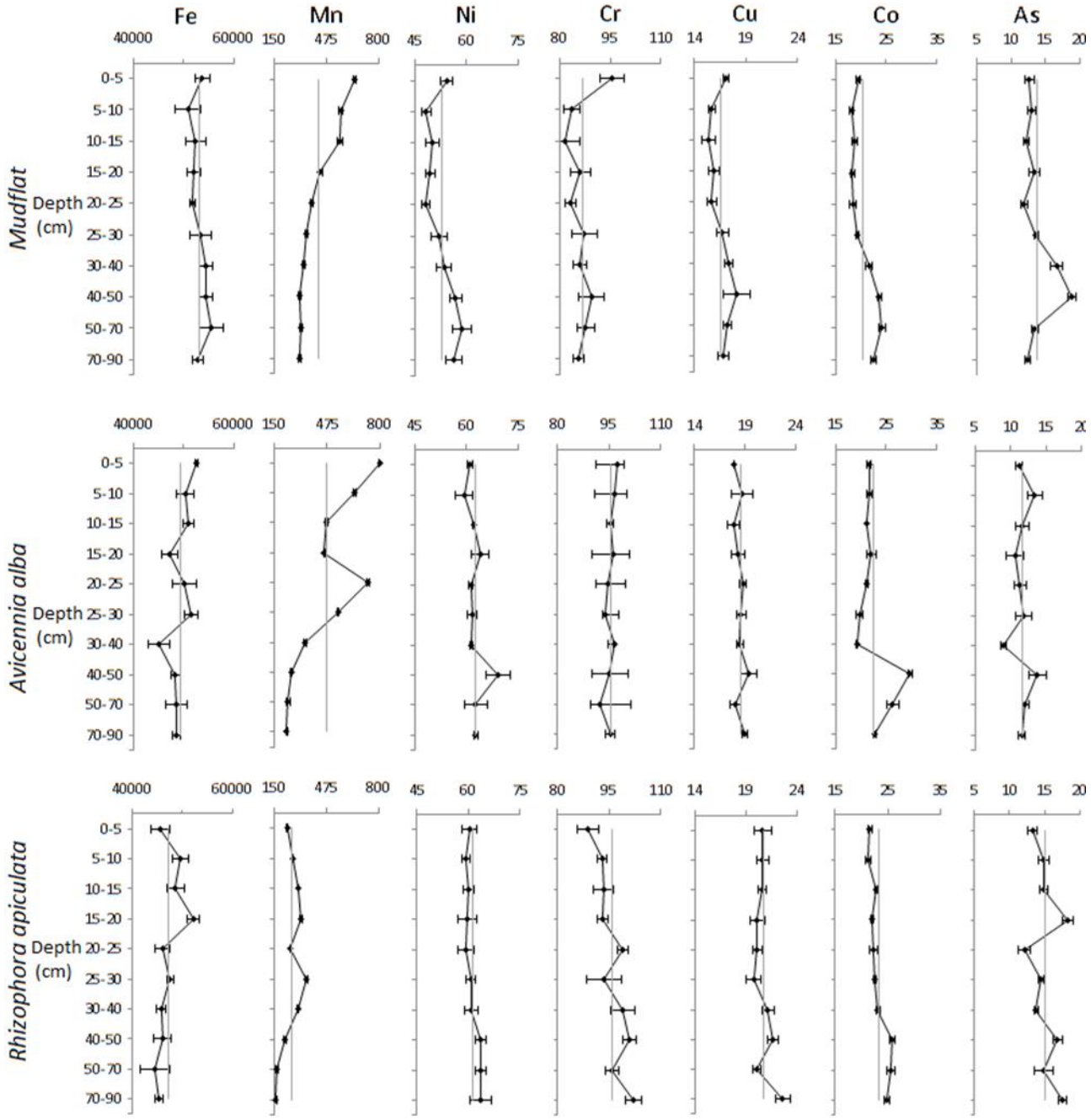

Fig. 3. Vertical distributions of metals concentrations (square dots) in the mudflat, the Avicennia stand and the Rhizophora stand (expressed in mg kg^{-1}), with gray line presenting mean metal concentrations of each core.

3.3. *Metal stock estimation*

The metal stocks were estimated over the 50 cm depth profile of the cores. Interestingly, the metal stocks differed between the mangrove stands and the mudflat (Table 2). The Fe stock

presented decreasing values from the mudflat (169.2 ± 4.2 t ha^{-1}) to the inner mangrove (i.e. the *Rhizophora* stand, 126.4 ± 6.2 t ha^{-1}). Conversely, the stock of Mn was higher beneath the *Avicennia* stand (1.62 ± 0.57 t ha^{-1}) than in the mudflat (1.44 ± 0.41 t ha^{-1}) and was even lower in the *Rhizophora* stand (0.74 ± 0.12 t ha^{-1}). Except As stock, which was higher in the mudflat, the stocks of Co, Ni, Cr and Cu showed higher values in the *Avicennia* stand than in the *Rhizophora* zone and in the mudflat. They varied (expressed in t ha^{-1}) from 0.16 ± 0.004 to 0.19 ± 0.01 for Ni, from 0.25 ± 0.01 to 0.29 ± 0.003 for Cr, and from 0.053 ± 0.003 to 0.057 ± 0.002 for Cu, from 0.060 ± 0.004 to 0.067 ± 0.010 for Co, from 0.035 ± 0.005 to 0.045 ± 0.008 for As.

Table 2. Metal stocks in the sediments of the mudflat, the Avicennia stand and the Rhizophora stand in the Can Gio Mangrove (expressed in t ha^{-1}, values were obtained based on the average total metal concentration and average bulk density of each core on 50 cm depth). The metal stocks beneath Avicennia and Rhizophora stands were compared with those measured in the mudflat (%).

Stand	Bulk density (g cm^{-3})	Fe	Mn	Ni	Cr	Cu	Co	As
Mud flat	0.64	169.2 ± 4.2	1.44 ± 0.41	0.16 ± 0.01	0.28 ± 0.01	0.053 ± 0.003	0.063 ± 0.006	0.045 ± 0.008
Avicennia	0.61	150.9 ± 7.5	1.62 ± 0.57	0.19 ± 0.01	0.29 ± 0.003	0.057 ± 0.002	0.067 ± 0.010	0.035 ± 0.005
(% mud flat)		89	112	116	105	107	106	79
Rhizophora	0.53	126.4 ± 6.2	0.74 ± 0.12	0.16 ± 0.004	0.25 ± 0.01	0.055 ± 0.002	0.060 ± 0.004	0.039 ± 0.005
(% mud flat)		75	51	97	91	103	95	87

3.4. Metal partitioning in the sediment cores

The metals (Fe, Mn, Ni, Cr, Cu, Co and As) partitioning in each layer of sediment core collected in the mudflat, the *Avicennia* stand and the *Rhizophora* stand was determined based on their concentrations in the exchangeable/carbonate fraction (F1), the oxides fraction (F2), the organic fraction (F3) and the residual fraction (F4). Their respective percentages/ proportions in each phase were evaluated based on their total concentrations (i.e. summing of metal concentrations in four fractions), being presented in Fig. 4.

3.4.1. Fe and Mn

The Fe and Mn partitioning exhibited different vertical distributions according to environments. In the mudflat and in the *Avicennia* stand, the Fe partitioning was F4 > F2 > F3 ~ F1 (Fig. 4a) whereas for Mn it was: F4~ F1 > F2 > F3 (Fig. 4b). Fe in F4 was stable with depth, representing 72 % in the mudflat and 78 % in the *Avicennia* stand, whereas Mn in F4 increased with depth, from 22 % to 38 % in the mudflat and from 18 % to 62 % in the *Avicennia* stand. Mn was characterized

by an important exchangeable/carbonate fraction, which decreased from 42 % to 27 % in the mudflat and from 51 % to 22 % in the *Avicennia* stand. F2 of both Fe and Mn decreased with depth in the mudflat and in the *Avicennia* stand, respectively from 20 % to 12 % and 20 % to 12 % for Fe, and respectively from 42 % to 27 % and 51 % to 22 % for Mn. F3 of Fe and Mn presented increasing values with depth in the mudflat, from 8 % to 15 % for Fe and from 6 % to 13 % for Mn, while it is stable in the *Avicennia* stand with a mean value of 3 % for Fe and values ranging from 2 % to 6 % for Mn. F1 of Fe was stable with depth with mean values of 2 % and 3% in the mudflat and in the *Avicennia* stand, respectively.

In the *Rhizophora* stand, Fe and Mn exhibited the same partitioning: F4 > F3 > F2 > F1. The residual fraction was stable from the top to the 40 cm depth, and then gradually increased with depth from 62 % to 78 % for Fe and from 35 % to 66 % for Mn. The organic fraction of both Fe and Mn was higher in the *Rhizophora* stand than in the *Avicennia* stand and the mudflat. Conversely to F4, the proportion of Fe and Mn in F3 increased from the top to 40 cm depth (i.e. ranging from 18 to 36 % for Fe and 21 to 54 % for Mn), then decreased to the bottom of the core (i.e. ranged from 35 to 16 % and from 52 to 17 % for Fe and Mn, respectively). Fe and Mn in F2 decreased toward the bottom of the core, from 15 % to 3 % for Fe and from 23 % to 8 % for Mn. Eventually, the exchangeable/carbonate fraction of Fe represented less than 1 % of total Fe concentrations, while F1 of Mn decreases with depth from 16 % to 3 %.

3.4.2. Ni, Cr, Cu, Co and As

The Ni partitioning was characterized by F4 > F2 ~ F3 > F1 in the mudflat and the *Avicennia* stand and by F4 > F3 > F2 > F1 in the *Rhizophora* stand (Fig. 4c). F4 was in the same range (from 76 % to 84 %) in the mudflat and in the *Rhizophora* stand, but higher (from 83 % to 91 %) in the *Avicennia* stand, without clear vertical distributions in all cores. F3 was stable with depth and presented a higher proportion in the *Rhizophora* stand (11 %) than in the mudflat (8 %) and in *Avicennia* stand (5 %). F2 and F1 were stable with depth at all sites, and represented less than 8 % for F2 and less than 3 % for F1.

The Cr partitioning was F4 > F3 > F2 > F1, without any clear depth evolution (Fig. 4d). The residual fraction ranged from 78 % and 84 % in the mudflat and the *Avicennia* stand and from 72 % to 79 % in the *Rhizophora* stand. The organic fraction was characterized by higher proportion in the *Rhizophora* stand (16 % to 24 %) than in the mudflat (11 % to 17 %) and in the *Avicennia* stand (10 % to 13 %). The oxides fraction and the exchangeable/carbonate fraction presented low proportion (less than 5 %) and same range of values in all environments.

The Cu partitioning differed between sites: F4 > F3 > F1 > F2 in the mudflat, F4 > F3 > F2 ~ F1 in the *Avicennia* stand, and F4 > F3 > F2 > F1 in the *Rhizophora* stand (Fig. 4e). For the F4, the proportion of Cu was higher in the *Avicennia* stand (85 % to 94 %) than in the *Rhizophora* stand (44 % to 73 %) and in the mudflat (57 % to 75 %). In the mudflat, the proportion of Cu in F4 decreased with depth while no specific distribution was observed beneath the mangrove stands. F3 ranged from 24 % to 41 % in the mudflat and *Rhizophora* stand, and from 6 % to 14 % in the *Avicennia* stand. F1 and F2 fractions were characterized by low proportion (< 2 %) in all environments except in the *Rhizophora* stand where the F2 increased from 20 cm depth until the bottom of the core.

The Co partitioning also differed between cores: F4 > F2 ~ F3 > F1 in the mudflat, F4 > F2 > F1 ~ F3 in the *Avicennia* stand and F4 > F3 > F2 > F1 in the *Rhizophora* stand (Fig. 4f). The residual fraction was closed to 50 % in both the mudflat and the *Rhizophora* stand, but ranging from 50 % to 76 % in the *Avicennia* stand with lower proportion at depth. F3 presented opposite pattern than F4 in the mudflat and the mangrove stands. F2 and the F1 were stable in all environments with lower proportion in the *Rhizophora* stand for F2 and increasing F1 proportion from 40 cm depth in the *Avicennia* stand.

The As partitioning was F4 > F2 > F3 > F1 in the mudflat, F4 > F2 > F3 ~ F1 in the *Avicennia* stand and F4 > F2 ~ F3 > F1 in the *Rhizophora* stand (Fig. 4g). In the upper part of the core in the mudflat (to 25 cm depth), all fractions presented stable proportions. Then, As in F3 and F4 increased with depth while As in F1 and F2 decreased. In the core beneath the *Avicennia* stand, As proportion in F4 gradually decreased from the top to the 40 cm depth and dramatically increased

360 in deeper layers while the opposite distribution was observed for F3. F2 and F1 did not exhibit any
361 specific distribution along the core. In the *Rhizophora* stand, the residual and the organic fractions
362 were stable from the top of the core to 40 cm depth, then F4 increased toward the bottom while F3
363 decreased. The F2 and F1 fraction did not exhibit any specific distribution along the core.

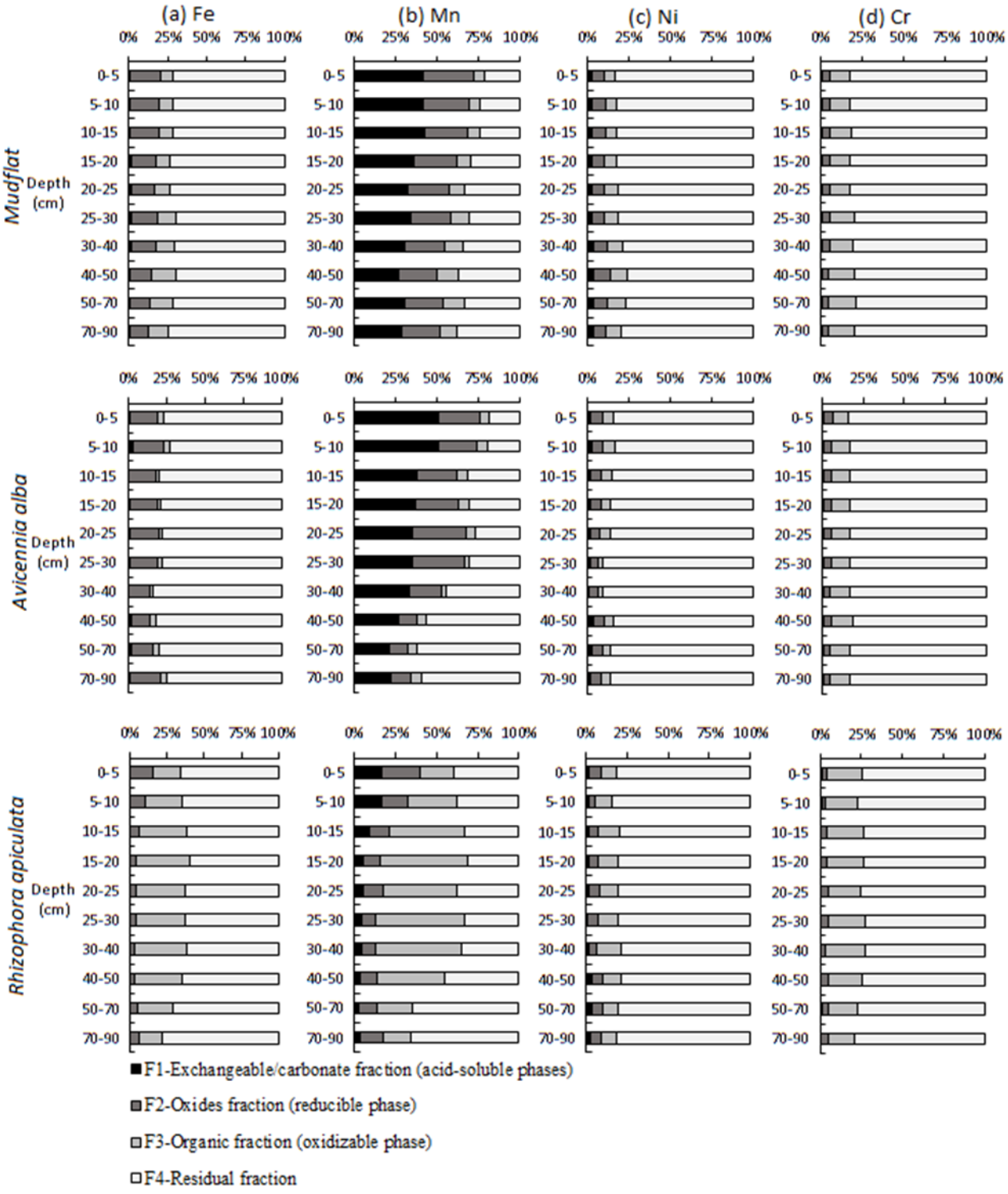

364

365 *Fig. 4. Depth profile of sequential extraction of (a) Fe, (b) Mn, (c) Ni, (d) Cr, (e) Cu, (f) Co and (g) As in the*
366 *mudflat, the Avicennia stand and the Rhizophora stand in the Can Gio Mangrove (to be continued).*

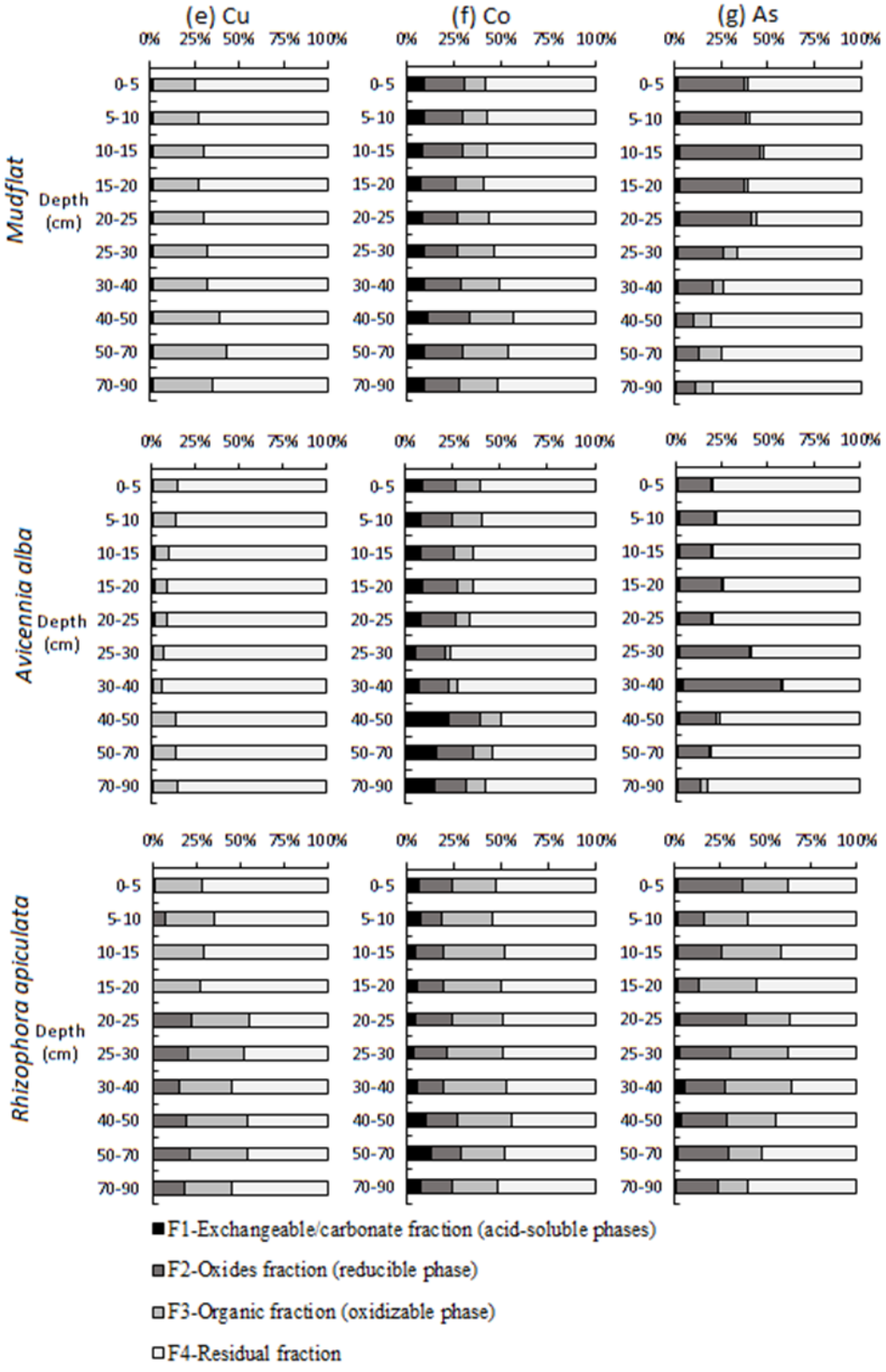

Fig. 4. (Continued)

3.5. *Dissolved metal concentrations in the core's pore-waters*

372 Dissolved Fe concentrations (Fe_D) in pore-waters presented lower level of concentration in the
373 *Rhizophora* stand (14 to 3,055 µg L^{-1}) and the mudflat (1,621 to 10,303 µg L^{-1}) than in the *Avicennia*
374 stand (333 to 40,771 µg L^{-1}). The Fe_D distributions were characterized by decreasing Fe_D from the
375 surface to 15 cm depth and then increasing values with depth in the stands (Fig. 5a). Dissolved Mn
376 concentrations (Mn_D) presented higher levels in the mudflat (from 6,812 to 15,106 µg L^{-1}) and in
377 the *Avicennia* stand (25 to 13,648 µg L^{-1}) than in the *Rhizophora* stand (from 542 to 643 µg L^{-1})
378 (Fig. 5b). The Mn_D concentrations decreased from the top to 10 cm depth (in *Avicennia* stand) and
379 to 40 cm depth (in *Rhizophora* stand) and then increased again with depth.
380 The dissolved Ni (Ni_D), Cr (Cr_D) and Cu (Cu_D) concentrations in pore-waters presented similar
381 patterns in the three cores (Fig. 5c, 5d and 5e). In the mudflat and the *Avicennia* stand, Ni_D, Cr_D
382 and Cu_D were stable with depth with increasing concentrations at 30 cm depth in the mudflat and
383 at 15 cm depth in the *Avicennia* stand. In the *Rhizophora* stand, Ni_D, Cr_D and Cu_D presented higher
384 concentrations with a decreasing pattern from the top to the surface for Ni_D and Cu_D and a stable
385 pattern with two peaks at 15 cm and 30 cm depth for Cr_D. The dissolved Co (Co_D) and As (As_D)
386 concentrations in pore-waters (Fig. 5f, 5g) presented a stable vertical distribution with a peak at 30
387 cm in the mudflat core while in the *Avicennia* stand, they presented decreasing concentrations from
388 the top to 10 cm depth, increasing concentrations until reaching a peak at 30 cm and 40 cm depth
389 for Co_D and As_D respectively, and then decreasing concentrations towards the bottom. Finally in
390 the *Rhizophora* stand, Co_D decreased with depth with a peak at 15 cm depth while As_D is stable
391 with two peaks at 25 cm and 50 cm depth.

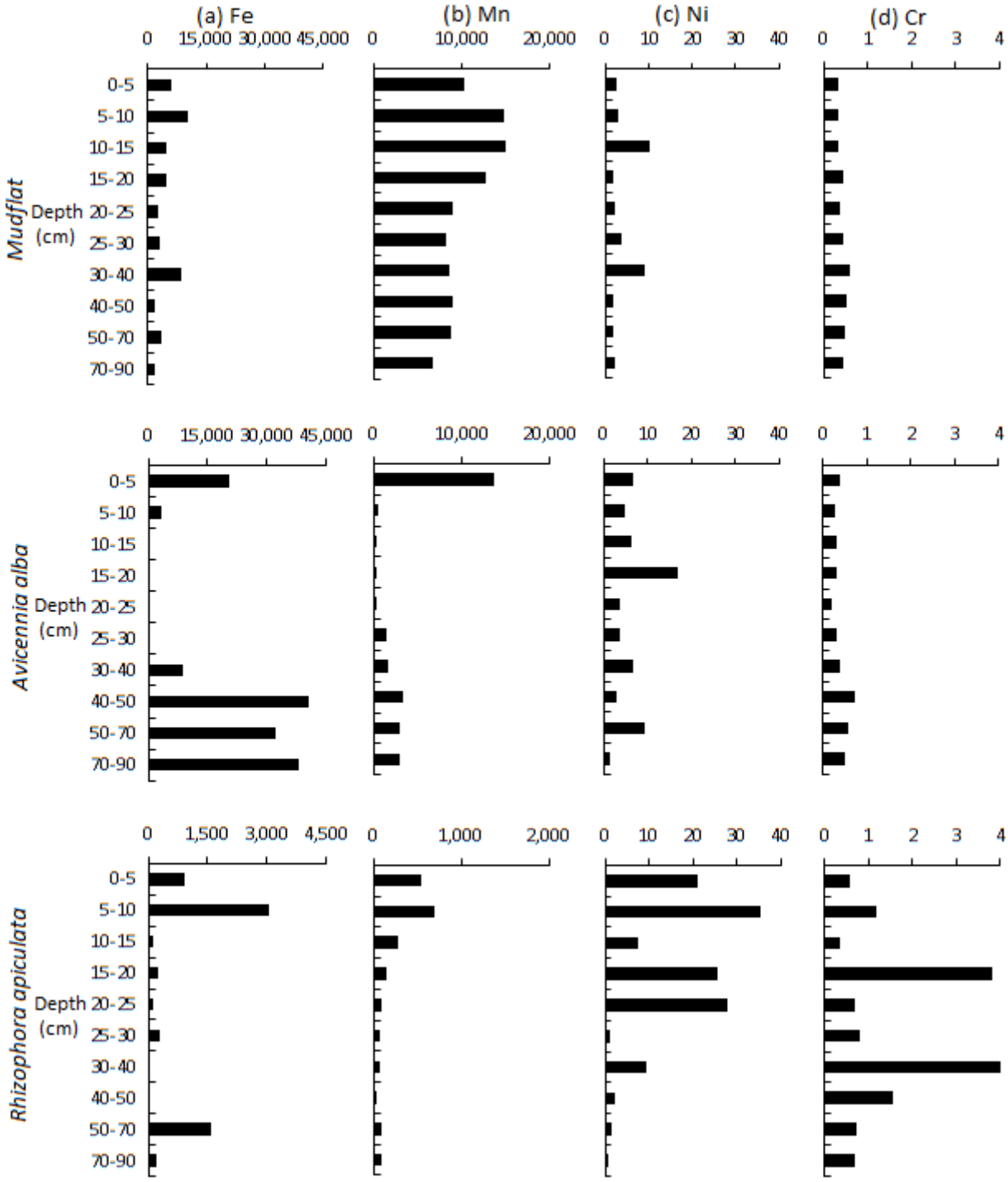

392

393 *Fig. 5. Depth profile of dissolved metals concentrations (µg L^{-1}) in the pore-waters of the mudflat, Avicennia and*

394 *Rhizophora stands. Asterisks highlight extreme values that could not be shown in the graph even with cut axis (i.e.*

395 *values of 14.4 for Cr and 13.9 for Cu) (to be continued).*

396

397

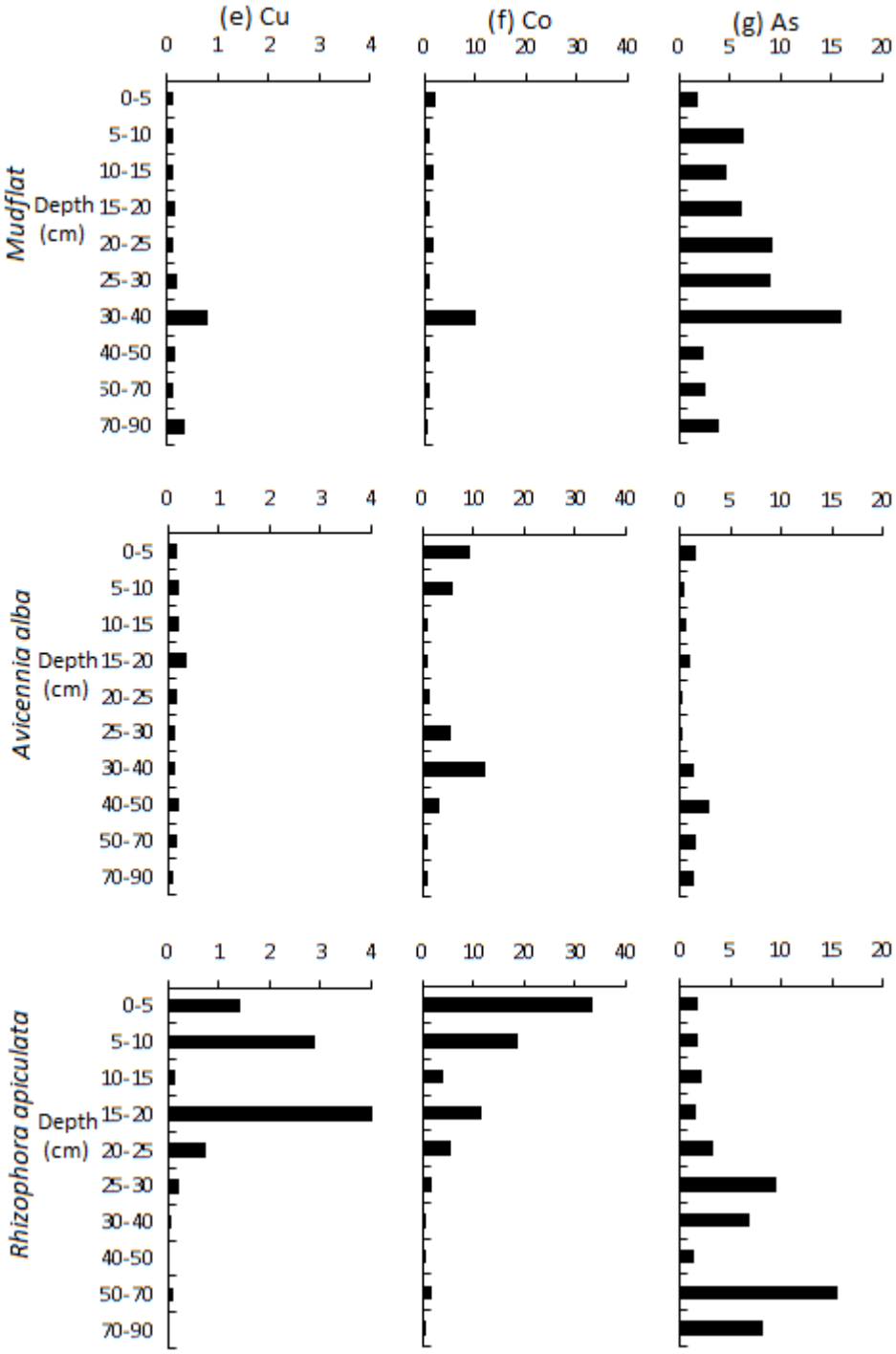

Fig. 5. (Continued)

4. Discussions

4.1. Mangrove sediments characteristics

Mangrove forests are known to be highly productive ecosystems (Bouillon et al. 2008), storing huge quantity of carbon in their sediments. Kristensen et al. (2008a) showed that TOC values in mangrove sediments usually range between 0.5 % and 15 %, with a median value around 2.2 %. In the Can Gio Mangrove, TOC reached up to 4.6 % with increasing values from the tidal creek (the

406 mudflat core) to the inner mangrove (the *Rhizophora* stand core) (Fig. 2). The higher values
407 measured beneath the *Rhizophora* stand than beneath the *Avicennia* stand may result from a higher
408 productivity of the first species, including a more developed root system as it was observed in
409 Australia (Alongi et al. 2000) or in New Caledonia (Marchand et al. 2011b). It may also be related
410 to the elevation of the sediment: the *Avicennia* trees in the Can Gio Mangrove developing at lower
411 elevation than the *Rhizophora* ones may thus be subject to a more intense tidal export of leaf litter,
412 which limits organic matter accumulation in the sediment. Additionally, the oxygen released by the
413 roots of *Avicennia* trees may induce more efficient organic matter decomposition (Marchand et al.
414 2004). Beneath the two mangrove stands, the redox values decreased with depth probably as a result
415 of organic matter decay and the lack of electron acceptors renewal at depth (Otero et al. 2009). In
416 the upper part of the sediments, the suboxic condition ($100 < Eh < 260$ mV) may be explained by
417 biological or physical factors (i.e. length of emersion, crab activity and bioturbation by mangrove
418 roots) (Marchand et al. 2012). The radial cable roots of *Avicennia* trees can also be important factor
419 inducing higher Eh values than in the *Rhizophora* stand (Marchand et al. 2004). Whereas the
420 mudflat is flooded almost all the time, the absence of air diffusion into the sediment can result to
421 anoxic condition despite its low organic content. We suggest that more intense organic
422 decomposition and possible sulfide oxidation may cause lower pH in the *Avicennia* stand than in
423 the *Rhizophora* stand and in the mudflat (Marchand et al. 2004). Finally, the upper sediment of
424 every core was characterized by lower salinity values than deeper sediment, which can be related
425 to the period of coring, i.e. the end of the wet season, the rainwater inducing a dilution of the saline
426 pore-waters. The rainwater may also be responsible of an enhanced renewal of electron acceptors,
427 influencing OM diagenesis.

428 *4.2. Lateritic soil as a main source of trace metal in the mangrove sediments.*

429 Mean metal concentrations (Fe, Mn, Ni, Cr, Co, Cu and As) in the Can Gio Mangrove sediments
430 (supplementary data, Fig. 3) are in the range of other mangroves around the world (see review
431 papers of Lewis et al. (2011) and Bayen (2012)) but are lower than those measured in mangroves
432 subject to strong anthropogenic pressure as in India (Fernandes and Nayak 2012). Furthermore,

these metal concentrations were also close to those measured in total suspended matter (TSM) in the Can Gio Mangrove Estuary (Thanh-Nho et al. 2018). These authors stated that TSM acted as main carrier for metals during their transport to the ocean, and that metal distribution changed due to the physical mixing by the seawater and/or organic matter decay processes. Consequently, most metal concentrations in TSM collected in the estuary were lower than upstream, specifically during the monsoon. We suggest that despite being downstream of a developing megacity characterized by low urban wastewater treatments (only 10 %, (FAO 2014)), metal accumulation inside the mangrove forest was relatively limited. Thus, we consider that the main source of metals in the Can Gio Mangrove is natural and originates from the rivers' watershed in the Central Highland of Vietnam, composed of lateritic soil originating from the physico-chemical weathering processes of basaltic rocks (Egawa and Ooba 1963) rich in hematite and goethite minerals. This hypothesis may be supported by the high proportion of metals in the residual fraction (Fig. 4) and interrelationships of total metals concentrations in the mudflat, which reflect sediment inputs without the influences of mangrove trees (Table 3).

Table 3. Pearson correlation matrix of total metal concentrations together in the mangrove mudflat. Metal concentrations were expressed in mg kg^{-1}.

	Fe	Mn	Ni	Cr	Cu	Co	As
Fe	1						
Mn	-.476	1					
Ni	.875**	-.483	1				
Cr	.538	.155	.544	1			
Cu	.842**	-.495	.854**	.674*	1		
Co	.831**	-.673*	.936**	.300	.828**	1	
As	.537	-.447	.424	.271	.757*	.562	1

**. Correlation is significant at the 0.01 level (2-tailed).

*. Correlation is significant at the 0.05 level (2-tailed).

4.3. Trace metal geochemistry in the sediment cores.

4.3.1. Redox sensitive elements (Fe and Mn)

Iron geochemistry

As suggested earlier, the erosion of lateritic soils upstream the Can Gio Mangrove may induce the transfer of these Fe-oxyhydroxides towards the estuary and then their deposition in the mangrove. In the main channel of the Can Gio Estuary, we measured iron concentration up to 55,302 mg kg^{-1} during the monsoon (Thanh-Nho et al. 2018), which comfort our hypothesis. However, in mangrove sediments, the oxide fraction was not the dominant one. This may be attributed first to the limitation of the selective extraction method offered by Tessier et al. (1979), which is inefficient to extract iron from highly crystallized oxides and oxyhydroxides, like iron crystalized forms e.g. ferrihydrite or lepidocrocite (Ferreira et al. 2007), and which may explain the dominance of the residual fraction. In the studied mangrove sediments, Fe partitioning in sediments and Fe_D concentrations varied with depth and between stands (Fig. 4a and 5a), which could result from the different redox conditions and driven by OM decomposition, bioturbation or root system activities. Iron partitioning beneath the *Avicennia* stand and the mudflat was similar, but the one beneath the *Rhizophora* stand was different and showed higher Fe concentrations in the oxidizable fraction but lower dissolved iron concentrations and lower Fe concentrations in residual, reducible and exchangeable/carbonate bound fractions. Thus, as Fe can form stable chelate complexes with organic matter (Thamdrup 2000), the increase of TOC in anoxic condition which were observed toward the landside of the mangrove could be responsible of the increasing Fe binding with organic phases in the mangrove sediment (Chakraborty et al. 2016). This phenomenon could be affirmed by negative correlation of Fe proportion in the oxidizable fraction with those in the reducible and the residual phases ($r = - 0.67$ and $- 0.85$, Fig. 6a and 6b respectively). We also suggest that Fe-oxihydroxydes originating from the lateritic soil of the watersheds were dissolved during diagenetic processes because of increased organic content (Froelich et al. 1979) and that the dissolved iron was subsequently complexed with OM as observed in other mangroves (Marchand et al. 2012). In anoxic conditions, Fe_D can also precipitate as sulphides, which can be reflected by the increased concentrations of Fe in the residual fraction at depth in the *Rhizophora* stand. Unfortunately, we were not able to measure neither total sulfur (TS) nor sulphide in the studied mangrove sediments. However, it is known that mangrove sediments are characterized by high rate of sulfate reduction

(Kristensen 2008b) and elevated TS content and pyrite are commonly observed in mangrove forest, especially at depth (Marchand et al. 2011a, Marchand et al. 2006). Eventually and in addition to these reduction processes, the re-oxidation of aqueous Fe(II) and pyrite could lead to the formation of poorly ordered ferrihydrite, lepidocrocite (c-FeOOH) and likely goethite (Noël et al. 2014) in the upper suboxic sediments, but cannot be confirmed with the selective extraction used.

Manganese geochemistry

Manganese is known as a highly redox sensitive element (Lacerda et al. 1999). Like for Fe, the presence of Mn_D in the pore-waters may result from the reductive dissolution of Mn-oxyhydroxides during the diagenetic processes (Froelich et al. 1979). This process can be responsible for the presence of high Mn_D concentrations in pore-waters, reaching more than 10,000 µg L^{-1} in the mudflat (Fig. 5b). The lower Mn_D observed in the *Avicennia* and *Rhizophora* stands than in the mudflat sediments may be related (i) to the loss of Mn_D by tidal drainage (Lacerda et al. 1999), Mn_D release from mangrove pore-waters being as a significant component of Mn oceanic budget (Holloway et al. 2016), (ii) to an uptake by mangrove plants (Wang et al. 2002), or iii) to more intense reprecipitation of Mn with other bearing phases after oxyhydroxides dissolution. We suggest that those processes were more pronounced for the *Rhizophora* stand, with 5-fold lower in mean concentration of dissolved Mn than those in the *Avicennia* stand (Fig. 5b). However and conversely to Fe, the dominant Mn fraction was the carbonate one in the two mangrove stands. Unlike Fe, Mn sulphides are unstable (pK_{sp} = 1.3) and the precipitation of Mn as sulphides may be severely limited by the presence of dissolved Fe^{2+} and carbonate. Because of similar ionic radii, Ca can be substituted by Mn in carbonate minerals (Costa-Boddeker et al. 2017, Rath et al. 2009). Previous studies, e.g. concerning mangrove sediments in the West coast of India (Noronha-D'Mello et al. 2015) or in Brazilia (Otero et al. 2009), reported that a considerable quantity of the free manganese was associated with carbonate (i.e. up to 2.5 µmol g^{-1}). Marchand et al. (2008) suggested that the decomposition of organic matter in mangrove sediments leads to the production of dissolved inorganic carbon (DIC) that can migrate at depth, where carbonate minerals can precipitate because of the marked anoxic conditions that prevail there compared to the upper

suboxic layers. This carbonate precipitation can be a sink for some elements, including Mn. In the *Rhizophora* stand, within the organic rich-layers, oxidizable fraction was the predominant one for Mn, suggesting that Mn was adsorbed onto OM (Thamdrup 2000). This hypothesis may be supported by negative correlation between Mn concentrations in the oxidizable fraction with those in the reducible and in the residual phase (i.e. r = - 0.69 and – 0.79, Fig. 6c and 6d respectively).

4.3.2. Geochemistry of Cu, Ni, Cr, Co, and As

Copper geochemistry

Copper may be released in pore-waters upon OM decay processes and/or reductive dissolution of Fe-Mn oxyhydroxides under suboxic conditions. Cu is a chalcophile element, being easily chemisorbed on or incorporated in several minerals such as chalcopyrite ($CuFeS_2$), covellite (CuS) and malachite $Cu_2CO_3(OH)_2$ (Pickering 1986). However, chalcopyrite and malachite are not stable under acidic conditions, especially at pH values ranging from 5 to 6. Therefore, the high Cu concentrations in the residual fraction beneath the *Avicennia* stand (where pH values < 6), compared to the mudflat and the *Rhizophora* stand, may result from the intense precipitation of Cu as sulphides, mainly CuS and/or Cu_2S (Fernandes 1997, Morse and Luther 1999). In the Can Gio Mangrove sediment, the negative correlation observed between the organic fraction and the residual one whatever the sites (i.e. r = - 0.89, Fig. 6e), evidenced that the control of organic matter on Cu partitioning (Chakraborty et al. 2015, Marchand et al. 2016, Silva et al. 2014) subsequently induces the opposite trend of Cu concentrations in the other fractions (i.e. exchangeable/carbonate and oxides bound, Fig. 4e). We note that beneath the *Rhizophora* stand, Cu concentrations in the organic fraction were higher than in the two other sites (Fig. 4e). Interestingly, the Cu_D in the three cores are in the same range than those measured in the Can Gio Mangrove Estuary surface water (Thanh-Nho et al. 2018). Cu is known to be an essential element for plant growth (Yruela 2009) and to bioaccumulate up to a bioconcentration factors of 9 in leaves and 5 in roots of mangrove trees (MacFarlane et al. 2003, Usman et al. 2013). Therefore, its low contents in pore-waters in addition to its precipitation with OM and sulphides may be related to its uptake by the mangroves root systems (Chakraborty et al. 2014, MacFarlane and Burchett 2002). However, some peaks of

increasing Cu_D are observed at 5 cm, 10 cm and 20 cm depth (1.4 µg L^{-1} 2.9 µg L^{-1} and 13.8 µg L^{-1}, respectively) in the *Rhizophora* stand (Fig. 5e), which may be attributed to a limited re-precipitation with oxides-bearing and supported by the Cu decreasing in the oxides fraction at these layers (Fig. 4e).

Nickel and Chromium geochemistry

The high proportions of Ni and Cr in the residual fractions from the mudflat to the inner mangrove stands may be attributed to more intense precipitation of Ni pyrite and/or Ni sulphide (Clark et al. 1998, Noël et al. 2015), reflecting their natural sources linked to iron minerals. This hypothesis could be supported by positive correlation between Ni, Cr and Fe proportions in the residual fractions respectively (r = 0.65 and 0.87, Fig. 6f and 6g). In the Can Gio Mangrove, the OM increase in the *Rhizophora* stand's sediment implies intense diagenetic processes which could lead to the formation of organocomplexes with dissolved Ni and Cr at the adequate pH (i.e. 3.4 % of mean TOC concentrations and pH ranging from 6.4 to 6.8). Doig and Liber (2006) demonstrated that the organonickel complexes may be formed at pH 6 to 8, which may explain the higher concentrations of Ni in the organic fraction beneath *Rhizophora* than beneath the two other stands (i.e. 11.4 % in the *Rhizophora* stand vs. 5.4 % in the *Avicennia* stand and 8.2 % in the mudflat, Fig. 4c). In fact, the variation of organic matter with depth in the *Rhizophora* stand induces the modification of Ni partitioning between bearing phases (e.g. a negative correlation was observed between Ni proportion in F3 and F4, r = - 0.6, Fig. 6h). Similar phenomenon was observed for Cr partitioning, being supported by a negative correlation between Cr proportion in F3 and F4 beneath the *Rhizophora* stand, r = - 0.96, Fig. 6i) like demonstrated in New Caledonia (Marchand et al. 2012). Lacerda et al. (1991) also observed in a Brazilian mangrove that Cr was immobilized in sediment as organochromium complexes.

Cobalt and Arsenic geochemistry

Conversely to Cu, Ni, and Cr, the concentrations of Co and As in the exchangeable/carbonate bound fraction were elevated, reaching up to 23 % and 5.4 % respectively. As explained earlier for Mn partitioning and the presence of Mn-carbonates, we suggest that the decomposition of organic

matter can lead to DIC production, which can precipitate in specific redox-pH values, incorporating some elements, mainly Mn but also Co and As. Co and Mn proportions in the exchangeable/carbonate fraction showed the opposite distribution patterns with depth whatever the sites (Fig. 4f) which implies considerable competition of dissolved Mn on the formation of carbonate cobalt (i.e. negative correlation observed in the mudflat, r = - 0.50, Fig. 6j; in the *Avicennia stand*, r = - 0.64, Fig. 6k). In fact, Co (III) can be substituted to Mn in Mn (III/IV) oxides because of their similar ionic radii, (Manceau et al. 1997). This process can occur in the same Eh-pH space in which Mn (II) oxidation occurs (Murray and Dillard 1979). However, it was not the case for Co behavior in the *Rhizophora* stand which may be attributed to the influence of OM. As a consequence, a negative correlation between the Co proportion in the residual fraction and the organic one was observed (r = - 0.83, Fig. 6l), which evidenced one more time the key role of organic matter in trace metal partitioning in mangrove sediments. Beneath the *Avicennia* stand, Co concentrations in the organic fraction were the lowest of the 3 stands despite similar range of TOC in the mudflat, which may result the precipitation of dissolved Co into sulphides forms (Charriau et al. 2011). In the case of As, we suggest that the increasing concentrations of As in the residual fraction with depth in every sites may result from the incorporation of As into pyrite. In fact, the most common iron sulphide minerals have strong affinity for, and can incorporate large amounts of arsenic in its structure, up to 10 wt % (Abraitis et al. 2004, Qiu et al. 2017). Noël et al. (2014) stated that pyrite was the predominant Fe bearing phase at depth in mangrove sediments. Notably, dissolved As concentrations were relatively high in the mudflat and at depth in the *Rhizophora* stand, reaching almost 20 µg L^{-1} (Fig. 5g). We suggest that the presence of As_D in pore-waters results from the reductive dissolution of As bound to oxides under suboxic/anoxic conditions (Masscheleyn et al. 1991, Nickson et al. 2000). Recent studies also supported that the reduction of Fe-oxyhydroxides was a cause of As release into ground water in Bangladesh (Anawar et al. 2003, Zheng et al. 2004).

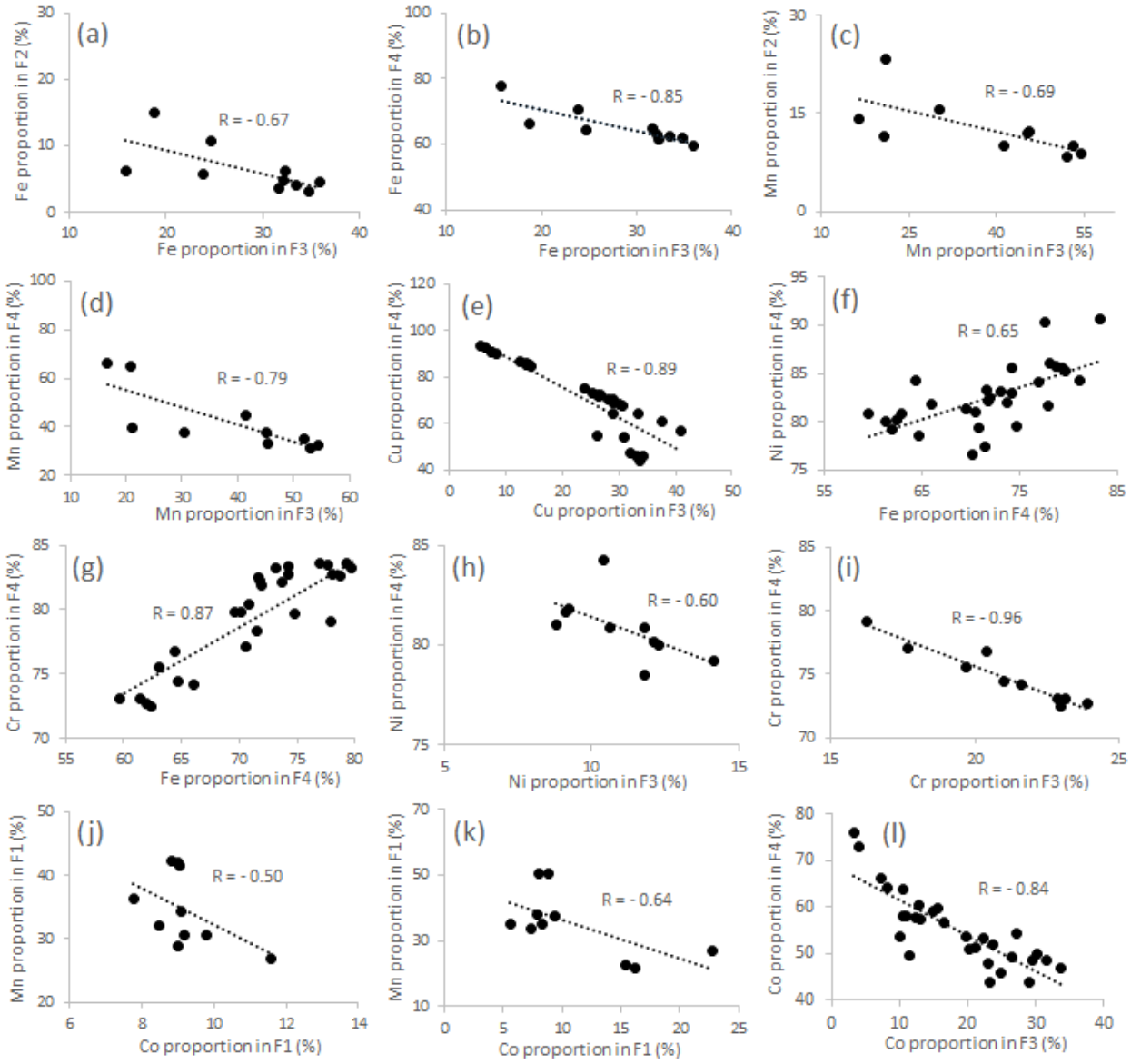

Fig. 6. Interrelationships of metals proportions in the different fractions of the sediment cores in Can Gio Mangrove: (a and b) Fe proportions beneath the Rhizophora stand; (c and d) Mn proportions beneath the Rhizophora stand; (e) data of Cu proportion beneath mangrove stands and mudflat; (f and g) Fe proportion in F4 correlated to Ni and Cr proportion in F4 of all sites from the mudflat to inner the Avicennia and Rhizophora stands, respectively; (h and i) Ni and Cr proportions beneath the Rhizophora stand; (j and k) Co and Mn proportions selected from the mudflat and the Avicennia stand, respectively; (l) Co proportions from all cores.

4.4. Assessment of metal stocks and ecological potential risks

The estimated metal stocks in the upper 50 cm sediment were lower in the *Rhizophora* stand compared to the *Avicennia* one and the mudflat and could be related to two processes. Firstly, the increase organic matter content in the sediment could induce a decrease in the bulk density of the sediments (0.55 g cm^{-3} in the *Rhizophora vs.* 0.61 g cm^{-3} in the *Avicennia* and 0.64 g cm^{-3} in the

mud flat). Secondly, it may be related to a more reactive substrate like described in the previous discussions, which can induce the dissolution of some bearing phases and the export of dissolved metals through pore-water seepage, or the uptake of dissolved metals by mangrove plants. Compared to mangrove of New Caledonia (Marchand et al. 2016), the estimated metal stocks of the Can Gio Mangrove sediments were lower confirming the moderate metal inputs in this system.

The bioavailability and potential toxicity of metals in the different geochemical fractions are expected to decrease in the following order: exchangeable/carbonate fraction > oxides fraction > organic fraction > residual fraction (Ma and Rao 1997). To assess the metal availability and associated potential ecological risks of the Can Gio Mangrove sediments, we used the Risk Assessment Code - RAC (Perin et al. 1985) and guideline (Benson et al. 2017, Passos et al. 2010) (Fig. 7).

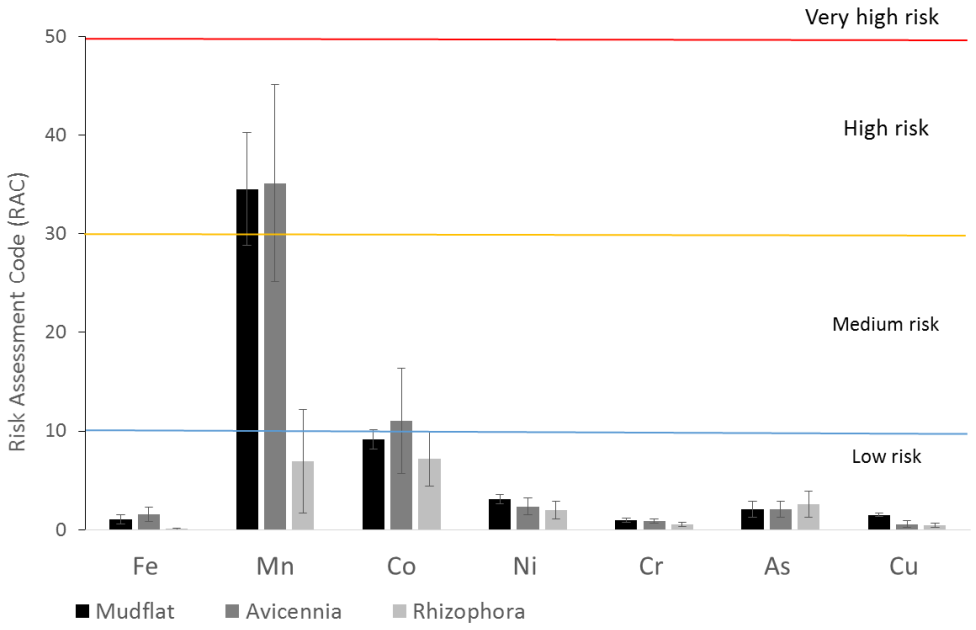

Fig. 7. Risk Assessment Code of metals in the sediment cores of the mudflat, the Avicennia stand and the Rhizophora stand in the Can Gio Mangrove.

The RAC is evaluated based on the percentage of metal concentrations that is representative in the bioavailable fraction (exchangeable/carbonate bound) to the total trace metal concentrations. According to the RAC guideline, metal with less than 1 % of exchangeable/carbonate fraction would be at no risk to the environment while higher ratio suggest: 1 % to 10 %: low risk; 11 % to 30 %: medium risk; 31 % to 50 %: high risk and > 50 %: very high risk. Consequently, in the Can

Gio Mangrove sediments, only Mn presented a high risk in the mudflat and in the *Avicennia* stand (i.e. RAC > 33) and a low risk in the *Rhizophora* stand (i.e. RAC < 7). We note that in plants, Mn excess can damage the photosynthesis apparatus (Millaleo et al. 2010) and thus the plants productivity (Nguyen et al. 2018). Arsenic presented a low risk but its high dissolved concentrations in pore-waters, reaching up to ~20 µg L^{-1}, may potentially be an additional ecological risk to organisms. Ni, Co, Fe, and Cu showed low risks to the ecosystem while Cr was in the no risk category whatever the sites. Along the mangrove, the RAC was lower in the *Rhizophora* stand than in the *Avicennia* stand and the mudflat, which may result from the competition of organometallic complexation (see earlier discussion), reflecting the important role of organic matter in scavenging metals in mangrove sediments. Eventually, as a result of mangrove conversion for agriculture and/or aquaculture (i.e. salt production and shrimp farming, etc.), these sediments may be subject to an oxidation resulting in enhanced OM decomposition (Grellier et al. 2017), sulphide oxidation, and thus sediments acidification. Noël et al. (2017) showed that increasing anthropogenic pressure on coastal areas altered the redox state of mangrove sediments from reducing condition to oxidizing condition, affecting the stability of Ni-accumulating Fe-sulfides and releasing significant dissolved metals at the redox boundary. Consequently, metals which were associated with OM and sulphides will be released in pore-waters, but also those associated with the exchangeable/carbonate bound due to the acidification, conducting all metals to be potentially at high ecological risks in the Can Gio Mangrove sediments.

5. Conclusions

The Can Gio Mangrove sediments did not present high metals concentrations. Their contents, close to those of the crust, associated with their high proportion in residual fractions suggested that studied metals originated from the lateritic soils of the Sai Gon and Dong Nai River watersheds. These metals were deposited mainly as Fe-Mn oxyhydroxides in the sediment, which were subsequently dissolved by bacteria in suboxic to anoxic conditions during diagenetic processes, releasing them in pore-waters. The OM enrichment in the sediments from the mudflat to the *Rhizophora* stand played a key role in metals partitioning, either because its decay modifies the

redox conditions (inducing oxyhydroxides dissolution and sulphides precipitation) or because of the formation of organometallic compounds. Most metals presented low ecological risks to the mangrove ecosystem except Mn, and possibly As due to its elevated dissolved concentrations. We would like to underscore that any anthropogenic perturbation in the redox state of those mangrove sediments may result in a release of metal contents in the adjacent ecosystems i.e. mangrove uptake or export to surface water. We suggest that a further detailed investigation on dissolved metal transfer and their accumulation into mangrove biota should be carried out to get a better understanding of metal dynamic in the Can Gio Mangrove ecosystem.

Acknowledgements

The authors would like to thank the students Nguyen Ngoc Hon and Nguyen Truong Giang for their help during sampling. This research is funded by Vietnam National University Ho Chi Minh City (VNU-HCM) under grand number C2016-18-07.

References

Abraitis P., Pattrick R. and Vaughan D. (2004). Variations in the compositional, textural and electrical properties of natural pyrite: a review. International Journal of Mineral Processing 74(1-4), 41-59.

Alongi D., Tirendi F. and Clough B. (2000). Below-ground decomposition of organic matter in forests of the mangroves Rhizophorastylosa and Avicenniamarina along the arid coast of Western Australia. Aquatic Botany 68(2), 97-122.

Anawar H. M., Akai J., Komaki K., Terao H., Yoshioka T., Ishizuka T., Safiullah S. and Kato K. (2003). Geochemical occurrence of arsenic in groundwater of Bangladesh: sources and mobilization processes. Journal of Geochemical Exploration 77(2-3), 109-131.

Babut M., Mourier B., Desmet M., Simonnet-Laprade C., Labadie P., Budzinski H., De Alencastro L. F., Tu T. A., Strady E. and Gratiot N. (2019). Where has the pollution gone? A survey of organic contaminants in Ho Chi Minh city / Saigon River (Vietnam) bed sediments. Chemosphere 217, 261-269.

Bayen S. (2012). Occurrence, bioavailability and toxic effects of trace metals and organic contaminants in mangrove ecosystems: a review. Environment International 48, 84-101.

Benson N. U., Udosen E. D., Essien J. P., Anake W. U., Adedapo A. E., Akintokun O. A., Fred-Ahmadu O. H. and Olajire A. A. (2017). Geochemical fractionation and ecological risks assessment of benthic sediment-bound heavy metals from coastal ecosystems off the Equatorial Atlantic Ocean. International Journal of Sediment Research 32(3), 410-420.

Blasco F., Aizpuru M. and Gers C. (2001). Depletion of the mangroves of Continental Asia. Wetlands Ecology and Management 9, 245-256.

Bouillon S., Borges A. V., Castañeda-Moya E., Diele K., Dittmar T., Duke N. C., Kristensen E., Lee S. Y., Marchand C. and Middelburg J. J. (2008). Mangrove production and carbon sinks: a revision of global budget estimates. Global Biogeochemical Cycles 22(2).

Chakraborty P., Chakraborty S., Jayachandran S., Madan R., Sarkar A., Linsy P. and Nath B. N. (2016). Effects of bottom water dissolved oxygen variability on copper and lead fractionation in the sediments across

682 the oxygen minimum zone, western continental margin of India. Science of The Total Environment 566,
683 1052-1061.
684 Chakraborty P., Chakraborty S., Ramteke D. and Chennuri K. (2014). Kinetic speciation and bioavailability
685 of copper and nickel in mangrove sediments. Marine Pollution Bulletin 88(1-2), 224-230.
686 Chakraborty P., Ramteke D. and Chakraborty S. (2015). Geochemical partitioning of Cu and Ni in mangrove
687 sediments: relationships with their bioavailability. Marine Pollution Bulletin 93(1-2), 194-201.
688 Charriau A., Lesven L., Gao Y., Leermakers M., Baeyens W., Ouddane B. and Billon G. (2011). Trace metal
689 behaviour in riverine sediments: Role of organic matter and sulfides. Applied Geochemistry 26(1), 80-
690 90.
691 Clark M. W., McConchie D., Lewis D. W. and Saenger P. (1998). Redox stratification and heavy metal
692 partitioning in Avicennia-dominated mangrove sediments: a geochemical model. Chemical Geology
693 149(3-4), 147-171.
694 Cormier-Salem M.-C., Van Trai N., Burgos A., Durand J.-D., Bettarel Y., Klein J., Duc Huy H. and Panfili J.
695 (2017). The mangrove's contribution to people: Interdisciplinary pilot study of the Can Gio Mangrove
696 Biosphere Reserve in Viet Nam. Comptes Rendus Geoscience 349(6-7), 341-350.
697 Costa-Boddeker S., Hoelzmann P., Thuyen L. X., Huy H. D., Nguyen H. A., Richter O. and Schwalb A. (2017).
698 Ecological risk assessment of a coastal zone in Southern Vietnam: Spatial distribution and content of
699 heavy metals in water and surface sediments of the Thi Vai Estuary and Can Gio Mangrove Forest.
700 Marine Pollution Bulletin 114(2), 1141-1151.
701 De Wolf H. and Rashid R. (2008). Heavy metal accumulation in Littoraria scabra along polluted and pristine
702 mangrove areas of Tanzania. Environmental Pollution 152(3), 636-643.
703 Dent D. (1986). Acid sulphate soils: a baseline for research and development, ILRI.
704 Doig L. E. and Liber K. (2006). Nickel partitioning in formulated and natural freshwater sediments.
705 Chemosphere 62(6), 968-979.
706 Duke N. C., Meynecke J.-O., Dittmann S., Ellison A. M., Anger K., Berger U., Cannicci S., Diele K., Ewel K. C.
707 and Field C. D. (2007). A world without mangroves? Science 317(5834), 41-42.
708 Egawa T. and Ooba Y. (1963). Mineralogical studies of some soils in the central highland of vietnam. Soil
709 Science and Plant Nutrition 9(6), 14-20.
710 FAO (2014). Aquastat: Global information system on water and agriculture.
711 www.fao.org/nr/water/aquastat/data/cf/readPdf.html?f=VNM-CF_eng.pdf.
712 Fernandes H. M. (1997). Heavy metal distribution in sediments and ecological risk assessment: the role of
713 diagenetic processes in reducing metal toxicity in bottom sediments. Environmental Pollution 97(3),
714 317-325.
715 Fernandes L. L. and Nayak G. N. (2012). Heavy metals contamination in mudflat and mangrove sediments
716 (Mumbai, India). Chemistry and Ecology 28(5), 435-455.
717 Ferreira T. O., Otero X. L., Vidal-Torrado P. and Macías F. (2007). Effects of bioturbation by root and crab
718 activity on iron and sulfur biogeochemistry in mangrove substrate. Geoderma 142(1-2), 36-46.
719 Froelich P. N., Klinkhammer G., Bender M. L., Luedtke N., Heath G. R., Cullen D., Dauphin P., Hammond D.,
720 Hartman B. and Maynard V. (1979). Early oxidation of organic matter in pelagic sediments of the
721 eastern equatorial Atlantic: suboxic diagenesis. Geochimica et Cosmochimica Acta 43(7), 1075-1090.
722 Grellier S., Janeau J. L., Dang Hoai N., Nguyen Thi Kim C., Le Thi Phuong Q., Pham Thi Thu T., Tran-Thi N. T.
723 and Marchand C. (2017). Changes in soil characteristics and C dynamics after mangrove clearing
724 (Vietnam). Science of The Total Environment 593-594, 654-663.
725 Holloway C. J., Santos I. R., Tait D. R., Sanders C. J., Rose A. L., Schnetger B., Brumsack H.-J., Macklin P. A.,
726 Sippo J. Z. and Maher D. T. (2016). Manganese and iron release from mangrove porewaters: A
727 significant component of oceanic budgets? Marine Chemistry 184, 43-52.
728 Hong P. N. (2001). Reforestation of mangroves after severe impacts of herbicides during the the Viet Nam
729 war: the case of Can Gio. Unasylva (FAO).
730 Kristensen E. (2008b). Mangrove crabs as ecosystem engineers; with emphasis on sediment processes.
731 Journal of Sea Research 59(1-2), 30-43.
732 Kristensen E., Bouillon S., Dittmar T. and Marchand C. (2008a). Organic carbon dynamics in mangrove
733 ecosystems: A review. Aquatic Botany 89(2), 201-219.

Kuenzer C. and Tuan V. Q. (2013). Assessing the ecosystem services value of Can Gio Mangrove Biosphere Reserve: Combining earth-observation- and household-survey-based analyses. Applied Geography 45, 167-184.

Kutscher D., Wills J. D. and McSheehy D. S. (2014). Analysis of High Matrix Samples using Argon Gas Dilution with the Thermo Scientifc iCAP Q ICP-MS. Technical Note 43202, Thermo Fisher Scientific, Bremen, Germany.

Lacerda L., Rezende C., Aragon G. and Ovalle A. (1991). Iron and chromium transport and accumulation in a mangrove ecosystem. Water, Air, and Soil Pollution 57(1), 513-520.

Lacerda L. D., Ribeiro Jr M. G. and Gueiros B. B. (1999). Manganese dynamics in a mangrove mud flat tidal creek in SE Brazil. Mangroves and Salt Marshes 3, 105-115.

Lee S. Y., Primavera J. H., Dahdouh-Guebas F., McKee K., Bosire J. O., Cannicci S., Diele K., Fromard F., Koedam N., Marchand C., Mendelssohn I., Mukherjee N. and Record S. (2014). Ecological role and services of tropical mangrove ecosystems: a reassessment. Global Ecology and Biogeography 23(7), 726-743.

Lewis M., Pryor R. and Wilking L. (2011). Fate and effects of anthropogenic chemicals in mangrove ecosystems: a review. Environmental Pollution 159(10), 2328-2346.

Luong N. V. (2011). Mangrove forest structure and coverage change analysis using remote sensing and geographical information system technology: A case study of Can Gio Mangrove Biosphere Reserve, Hi Chi Minh City, Vietnam. Final report submitted to Rufford Small Grants Foundation, 40pp.

Luong N. V., Tateishi R. and Hoan N. T. (2015). Analysis of an impact of succession in mangrove forest association using remote sensing and GIS technology. Journal of Geography and Geology 7(1), 106.

M. Brander L., J. Wagtendonk A., S. Hussain S., McVittie A., Verburg P. H., de Groot R. S. and van der Ploeg S. (2012). Ecosystem service values for mangroves in Southeast Asia: A meta-analysis and value transfer application. Ecosystem Services 1(1), 62-69.

Ma L. Q. and Rao G. N. (1997). Chemical fractionation of cadmium, copper, nickel, and zinc in contaminated soils. Journal of Environmental Quality 26(1), 259-264.

MacFarlane G. and Burchett M. (2002). Toxicity, growth and accumulation relationships of copper, lead and zinc in the grey mangrove Avicennia marina (Forsk.) Vierh. Marine Environmental Research 54(1), 65-84.

MacFarlane G., Pulkownik A. and Burchett M. (2003). Accumulation and distribution of heavy metals in the grey mangrove, Avicennia marina (Forsk.) Vierh.: biological indication potential. Environmental Pollution 123(1), 139-151.

MacKenzie R. A., Foulk P. B., Klump J. V., Weckerly K., Purbospito J., Murdiyarso D., Donato D. C. and Nam V. N. (2016). Sedimentation and belowground carbon accumulation rates in mangrove forests that differ in diversity and land use: a tale of two mangroves. Wetlands Ecology and Management 24(2), 245-261.

Manceau A., Silvester E., Bartoli C., Lanson B. and Drits V. A. (1997). Structural mechanism of Co2+ oxidation by the phyllomanganate buserite. American Mineralogist 82(11-12), 1150-1175.

Marchand C., Allenbach M. and Lallier-Vergès E. (2011b). Relationships between heavy metals distribution and organic matter cycling in mangrove sediments (Conception Bay, New Caledonia). Geoderma 160(3-4), 444-456.

Marchand C., Baltzer F., Lallier-Vergès E. and Albéric P. (2004). Pore-water chemistry in mangrove sediments: relationship with species composition and developmental stages (French Guiana). Marine geology 208(2-4), 361-381.

Marchand C., Fernandez J. M. and Moreton B. (2016). Trace metal geochemistry in mangrove sediments and their transfer to mangrove plants (New Caledonia). Science of The Total Environment 562, 216 - 227.

Marchand C., Fernandez J. M., Moreton B., Landi L., Lallier-Vergès E. and Baltzer F. (2012). The partitioning of transitional metals (Fe, Mn, Ni, Cr) in mangrove sediments downstream of a ferralitized ultramafic watershed (New Caledonia). Chemical Geology 300-301, 70-80.

Marchand C., Lallier-Vergès E. and Allenbach M. (2011a). Redox conditions and heavy metals distribution in mangrove forests receiving effluents from shrimp farms (Teremba Bay, New Caledonia). Journal of Soils and Sediments 11(3), 529-541.

Marchand C., Lallier-Vergès E. and Baltzer F. (2003). The composition of sedimentary organic matter in relation to the dynamic features of a mangrove-fringed coast in French Guiana. Estuarine, Coastal and Shelf Science 56(1), 119-130.
Marchand C., Lallier-Vergès E., Baltzer F., Albéric P., Cossa D. and Baillif P. (2006). Heavy metals distribution in mangrove sediments along the mobile coastline of French Guiana. Marine Chemistry 98(1), 1-17.
Marchand C., Lallier-Vergès E., Disnar J. R. and Kéravis D. (2008). Organic carbon sources and transformations in mangrove sediments: A Rock-Eval pyrolysis approach. Organic Geochemistry 39(4), 408-421.
Masscheleyn P. H., Delaune R. D. and Patrick Jr W. H. (1991). Effect of redox potential and pH on arsenic speciation and solubility in a contaminated soil. Environmental Science and Technology 25(8), 1414-1419.
Millaleo R., Reyes-Díaz M., Ivanov A., Mora M. and Alberdi M. (2010). Manganese as essential and toxic element for plants: transport, accumulation and resistance mechanisms. Journal of soil science and plant nutrition 10(4), 470-481.
Morse J. and Luther G. (1999). Chemical influences on trace metal-sulfide interactions in anoxic sediments. Geochimica et Cosmochimica Acta 63(19), 3373-3378.
Murray J. W. and Dillard J. G. (1979). The oxidation of cobalt (II) adsorbed on manganese dioxide. Geochimica et Cosmochimica Acta 43(5), 781-787.
Nguyen B. T., Do T. K., Tran T. V., Dang M. K., Dell C. J., Luu P. V. and Vo Q. T. K. (2018). High soil Mn and Al, as well as low leaf P concentration, may explain for low natural rubber productivity on a tropical acid soil in Vietnam. Journal of plant nutrition, 1-12.
Nguyen T. T. N., Nemery J., Gratiot N., Strady E., Tran V. Q., Nguyen A. T., Aime J. and Peyne A. (2018). Nutrient dynamics and eutrophication assessment in the tropical river system of Saigon - Dongnai (southern Vietnam). Science of The Total Environment 653, 370-383.
Nickson R., McArthur J., Ravenscroft P., Burgess W. and Ahmed K. (2000). Mechanism of arsenic release to groundwater, Bangladesh and West Bengal. Applied Geochemistry 15(4), 403-413.
Noël V., Juillot F., Morin G., Marchand C., Ona-Nguema G., Viollier E., Prévot F., Dublet G., Maillot F., Delbes L., Marakovic G., Bargar J. R. and Brown G. E. (2017). Oxidation of Ni-Rich Mangrove Sediments after Isolation from the Sea (Dumbea Bay, New Caledonia): Fe and Ni Behavior and Environmental Implications. ACS Earth and Space Chemistry 1(8), 455-464.
Noël V., Marchand C., Juillot F., Ona-Nguema G., Viollier E., Marakovic G., Olivi L., Delbes L., Gelebart F. and Morin G. (2014). EXAFS analysis of iron cycling in mangrove sediments downstream a lateritized ultramafic watershed (Vavouto Bay, New Caledonia). Geochimica et Cosmochimica Acta 136, 211-228.
Noël V., Morin G., Juillot F., Marchand C., Brest J., Bargar J. R., Muñoz M., Marakovic G., Ardo S. and Brown G. E. (2015). Ni cycling in mangrove sediments from New Caledonia. Geochimica et Cosmochimica Acta 169, 82-98.
Noronha-D'Mello, A. C. and Nayak G. N. (2015). Geochemical characterization of mangrove sediments of the Zuari estuarine system, West coast of India. Estuarine, Coastal and Shelf Science 167, 313-325.
Otero X. L., Ferreira T. O., Huerta-Díaz M. A., Partiti C. S. M., Souza V., Vidal-Torrado P. and Macías F. (2009). Geochemistry of iron and manganese in soils and sediments of a mangrove system, Island of Pai Matos (Cananeia — SP, Brazil). Geoderma 148(3-4), 318-335.
Parvaresh H., Abedi Z., Farshchi P., Karami M., Khorasani N. and Karbassi A. (2011). Bioavailability and concentration of heavy metals in the sediments and leaves of grey mangrove, Avicennia marina (Forsk.) Vierh, in Sirik Azini Creek, Iran. Biological trace element research 143(2), 1121-1130.
Passos E. d. A., Alves J. C., dos Santos I. S., Alves J. d. P. H., Garcia C. A. B. and Spinola Costa A. C. (2010). Assessment of trace metals contamination in estuarine sediments using a sequential extraction technique and principal component analysis. Microchemical Journal 96(1), 50-57.
Perin G., Craboledda L., Lucchese M., Cirillo R., Dotta L., Zanette M. and Orio A. (1985). Heavy metal speciation in the sediments of northern Adriatic Sea. A new approach for environmental toxicity determination. Heavy metals in the environment 2(1), 454-456.
Pickering W. (1986). Metal ion speciation—soils and sediments (a review). Ore Geology Reviews 1(1), 83-146.

Qiu G., Gao T., Hong J., Tan W., Liu F. and Zheng L. (2017). Mechanisms of arsenic-containing pyrite oxidation by aqueous arsenate under anoxic conditions. Geochimica et Cosmochimica Acta 217, 306-319.

Rath P., Panda U. C., Bhatta D. and Sahu K. C. (2009). Use of sequential leaching, mineralogy, morphology and multivariate statistical technique for quantifying metal pollution in highly polluted aquatic sediments--a case study: Brahmani and Nandira Rivers, India. Journal of Hazardous and Materials 163(2-3), 632-644.

Ross P. (1975). The mangroves of South Vietnam: the impact of military use of herbicides. Proceedings of the international symposium on biology and management of mangroves. Gainesville, Florida: Institute of Food and Agricultural Sciences, University of Florida.

Sanders C. J., Santos I. R., Barcellos R. and Silva Filho E. V. (2012). Elevated concentrations of dissolved Ba, Fe and Mn in a mangrove subterranean estuary: Consequence of sea level rise? Continental Shelf Research 43, 86-94.

Silva G. S. d., Nascimento A. S. d., Sousa E. R. d., Marques E. P., Marques A. L. B., Corrêa L. B. and Silva G. S. d. (2014). Distribution and Fractionation of Metals in Mangrove Sediment from the Tibiri River Estuary on Maranhão Island. Revista Virtual de Química 6(2).

Strady E., Dang V. B., Nemery J., Guedron S., Dinh Q. T., Denis H. and Nguyen P. D. (2017). Baseline seasonal investigation of nutrients and trace metals in surface waters and sediments along the Saigon River basin impacted by the megacity of Ho Chi Minh (Vietnam). Environmental Science and Pollution Research International 24(4), 3226–3243.

Tam N. and Wong Y. (1996). Retention and distribution of heavy metals in mangrove soils receiving wastewater. Environmental Pollution 94(3), 283-291.

Tessier A., Campbell P. G. and Bisson M. (1979). Sequential extraction procedure for the speciation of particulate trace metals. Analytical Chemistry 51(7), 844-851.

Thamdrup B. (2000). Bacterial manganese and iron reduction in aquatic sediments. Advances in microbial ecology, Springer**,** 41-84.

Thanh-Nho N., Strady E., Nhu-Trang T. T., David F. and Marchand C. (2018). Trace metals partitioning between particulate and dissolved phases along a tropical mangrove estuary (Can Gio, Vietnam). Chemosphere 196, 311-322.

Tuan V. Q. and Kuenzer C. (2012). Can Gio Mangrove Biosphere Reserve Evaluation 2012: Current status, Dynamics and Ecosystem Services Ha Noi, Viet Nam: IUCN, 102 pp.

Ure A. M., Quevauviller P., Muntau H. and Griepink B. (1993). Speciation of heavy metals in soils and sediments - an account of the improvement and harmonization of extraction techniques undertaken under the auspices of the BCR of the commission of the European comminities. International Journal of Environmental Analytical Chemistry 51(1-4), 135-151.

Usman A. R., Alkredaa R. S. and Al-Wabel M. I. (2013). Heavy metal contamination in sediments and mangroves from the coast of Red Sea: Avicennia marina as potential metal bioaccumulator. Ecotoxicology and Environmental Safety 97, 263-270.

Wang Z., Shan X.-q. and Zhang S. (2002). Comparison between fractionation and bioavailability of trace elements in rhizosphere and bulk soils. Chemosphere 46(8), 1163-1171.

Yruela I. (2009). Copper in plants: acquisition, transport and interactions. Functional Plant Biology 36(5), 409-430.

Zhang C., Yu Z. G., Zeng G. M., Jiang M., Yang Z. Z., Cui F., Zhu M. Y., Shen L. Q. and Hu L. (2014). Effects of sediment geochemical properties on heavy metal bioavailability. Environment International 73, 270-281.

Zheng Y., Stute M., Van Geen A., Gavrieli I., Dhar R., Simpson H., Schlosser P. and Ahmed K. (2004). Redox control of arsenic mobilization in Bangladesh groundwater. Applied Geochemistry 19(2), 201-214.